

Received May 13, 2019, accepted May 21, 2019, date of publication June 3, 2019, date of current version June 18, 2019.

Digital Object Identifier 10.1109/ACCESS.2019.2920418

# Novel Fuzzy Approximation Control Scheme for Flexible Air-Breathing Hypersonic Vehicles With Non-Affine Dynamics and Amplitude and Rate Constraints

XINGGE LI<sup>1</sup> AND GANG LI<sup>2</sup>

<sup>1</sup>Graduate College, Air Force Engineering University, Xi'an 710051, China

<sup>2</sup>Air and Missile Defense College, Air Force Engineering University, Xi'an 710051, China

Corresponding author: Xingge Li (lxg\_whut@126.com)

This work was supported in part by the Aeronautical Science Foundation of China under Grant 20175896023, in part by the National Natural Science Foundation of China under Grant 61603410, in part by the National Natural Science Foundation of China under Grant 61703424, and in part by the Natural Science Basic Research Plan in Shaanxi Province of China under Grant 2018JQ6024.

**ABSTRACT** This paper proposes a novel fuzzy control scheme for flexible air-breathing hypersonic vehicle (FAHV) non-affine models with amplitude and rate constraints. First, the non-affine dynamics of the FAHV is decomposed into velocity subsystem and altitude subsystem, then the non-affine models of each subsystem are converted into equivalent pure feedback forms, and the fuzzy approximator is used to estimate the total uncertainties of each subsystem. Since the input of control system can be limited by the actual actuator, a new error compensation auxiliary system is proposed to solve the amplitude and rate constraints of the actuator, and a fuzzy controller with auxiliary systems is designed. The stability of the closed-loop system is proved by the Lyapunov method. Through simulation verification, the effective performance of the control system has been proved.

**INDEX TERMS** Fuzzy approximator, flexible air-breathing hypersonic vehicle (FAHV), non-affine dynamics, error compensation auxiliary system, amplitude and rate constraints.

## I. INTRODUCTION

Flexible air-breathing hypersonic vehicles (FAHVs) are winged or wingless flight vehicles that fly in near space and fly at speeds greater than Mach 5 [1], [2]. FAHVs have the characteristics of wide flying range, fast flying speed and long flying distance, and because of their special design of engine/body integration, the fuselages are composed of flexible composite materials and the aerodynamic shapes are wave-riders, which make the control modes and dynamic characteristics of FAHVs very different from those of ordinary flight vehicles. For example, FAHV usually has obvious elastic vibration problem during flight. Serious elastic vibration will lead to instrumentation failure and flight vehicle disintegration. If the vibration of flexible body is not considered in the design of the controller, the control system may fail. At the same time, FAHVs have strong nonlinearity, fast time-varying, multi-coupling and uncertainties [3], [4].

The associate editor coordinating the review of this manuscript and approving it for publication was Lubin Chang.

Under the conditions of disturbance and uncertainties, a stable control system is utterly important. Furthermore, because FAHV is sensitive to attitude adjustment in high-speed flight, and in order to save fuels, they should take the initiative to avoid lateral maneuvers in flight process. Therefore, it is of great practical significance to research the longitudinal dynamics of FAHV. In recent years, the development of FAHVs is very rapid. Many advanced control strategies are applied to the longitudinal dynamics of hypersonic vehicles.

For hypersonic flight vehicles, there are extensive control theories and methods, such as robust control [5], [6], sliding mode control [7]–[9], back-stepping control [10] and funnel control [2], [11]. In recent years, intelligent control methods [12]–[14] are introduced into the FAHV control system. In the process of designing control laws for FAHVs, previous studies mainly focus on affine models and usually ignore the non-affine dynamics. Gao *et al.* [15] introduces fuzzy system into the subsystems of FAHV models, and estimating unknown functions online, but the algorithm requires that the unknown functions to be approximated are strictly positive

and bounded. In view of the uncertainties of system, [13] and [16] ignore some dynamic characteristics of FAHV, and design control laws based on strict feedback forms. However, the FAHVs' models are non-affine in the control inputs since the drag force  $D$  contains  $\delta_c^2$  [17], [18]. In [19], based on affine models, a robust controller based on dynamic inverse is designed, and the idea of back-stepping is applied in the controller. However, the back-stepping method requires numerous virtual control laws, which requires a high amount of computation. Buet *et al.* [20] proposes a control method based on non-singular neural network. The RBF neural network is used to approximate each unknown function in the subsystem, but the forms are cumbersome. Wang *et al.* [21] uses fuzzy system to estimate the unknown dynamics online, and a robust control law with adaptive gains is designed, which can achieve robust tracking of the reference inputs.

On the other hand, in the process of FAHVs maneuvering and flying, actuators are generally subject to constraints and limits. Fuel equivalence ratio is usually limited by the physical structure and working range of the engine. Especially when FAHVs are affected by unknown airflows such as gust and turbulence, the elevators are prone to saturation of amplitude and rate. When the actuators are saturated, the ideal control laws will be difficult to execute and even lead to control failure. Dong *et al.* [22], Dong *et al.* [23] proposes a reference switching system to ensure that the control inputs do not reach the restricted boundary. In [24], the tracking error of FAHV is modified by an auxiliary system, and the boundedness of the closed-loop system is proved, but the boundedness of the tracking error is not explained. An *et al.* [25] implement a novel anti-windup modification to handle the possible input saturation, but the effect is not obvious. Luo *et al.* [26] designs a control input conversion system that uses saturation functions to transform constrained control problems into unconstrained control problems. In [27], a finite-time disturbance observer is employed to estimate the lumped disturbance, while an auxiliary system combined with a command pre-filter is designed to analyze the effect of input saturation caused by the restrained actuators. Most of the previous studies focus on amplitude saturation, but the studies hardly deal with rate saturation. Therefore more researches are needed on rate saturation.

In view of the shortcomings of the above research, we propose an adaptive fuzzy controller with non-affine dynamics. A novel error compensation auxiliary system is proposed for the amplitude and rate constraints of the control system. First, the control system is decomposed into velocity subsystem and altitude subsystem. Based on uniqueness theorem of implicit function, we design a concise fuzzy controller for the velocity subsystem. For altitude subsystem, the non-affine models are transformed into equivalent pure feedback forms, and a fuzzy approximator is designed to approximate the unknown uncertainties. The stability of closed-loop system is proved by Lyapunov method. Finally, the effectiveness of the control method is verified by simulation analysis. The main advantages of this paper can be summarized as follows.

1. Compared with previous affine models, the proposed non-affine models avoid the loss of some key dynamics when the models are simplified.
2. The control scheme proposed in this paper does not need to design too many virtual control laws and define intermediate variables, which avoids the problem of "differential expansion" caused by multiple differentiation of virtual control laws.
3. Each subsystem contains only one fuzzy approximator, and introduces norm estimation approach [28], which reduces the amount of online calculation.
4. Compared with previous research, a new error compensation auxiliary system is proposed for amplitude and rate constraints problem of the system.

## II. PRELIMINARIES

### A. UNIQUENESS THEOREM OF IMPLICIT FUNCTION

*Lemma 1* [29]: If the implicit function  $G(\boldsymbol{\varpi}, \boldsymbol{\sigma}) \in \mathbf{R}^m$  with  $\boldsymbol{\sigma} \in \mathbf{R}^n$  satisfies the following conditions:

- (1)  $G(\boldsymbol{\varpi}, \boldsymbol{\sigma}) = 0$  is continuous in the region  $D \subset \mathbf{R}^{m \times n}$  with  $P_0(\boldsymbol{\varpi}_0, \boldsymbol{\sigma}_0)$  as the interior point;
- (2)  $G(\boldsymbol{\varpi}_0, \boldsymbol{\sigma}_0) = 0$ ;
- (3)  $(\partial G / \partial \boldsymbol{\varpi})(\boldsymbol{\varpi}, \boldsymbol{\sigma})$  and  $(\partial G / \partial \boldsymbol{\sigma})(\boldsymbol{\varpi}, \boldsymbol{\sigma})$  are continuous in region  $D$ ;
- (4)  $(\partial G / \partial \boldsymbol{\sigma})(\boldsymbol{\varpi}_0, \boldsymbol{\sigma}_0) \neq 0$ ;

In the region  $D$  of  $P_0$ , by  $G(\boldsymbol{\varpi}, \boldsymbol{\sigma}) = 0$ , it can uniquely obtain a function  $\boldsymbol{\sigma}_0 = g_0(\boldsymbol{\varpi}_0)$  defined on the neighborhood  $H \subset \mathbf{R}^m$ , and get  $G(\boldsymbol{\varpi}, g_0(\boldsymbol{\varpi})) = 0$ .

*Remark 1:* If the implicit function meets above 4 conditions,  $\boldsymbol{\sigma}$  can be expressed as a continuous differentiable function of  $\boldsymbol{\varpi}$ , i.e.,  $\boldsymbol{\sigma}_0 = g_0(\boldsymbol{\varpi}_0)$ . And then  $G(\boldsymbol{\varpi}, \boldsymbol{\sigma})$  can also be viewed as a continuous differentiable function of  $\boldsymbol{\varpi}$ . When  $\boldsymbol{\sigma}$  is difficult to obtain and  $G(\boldsymbol{\varpi}, \boldsymbol{\sigma})$  is an unknown function, a fuzzy approximator can be used to approximate  $G(\boldsymbol{\varpi}, \boldsymbol{\sigma})$ , and only  $\boldsymbol{\varpi}$  is needed as the input of the fuzzy system. According to this idea, we design the controller with non-affine dynamics.

### B. FUZZY APPROXIMATION THEORY

The advantage of fuzzy function is that we can effectively use fuzzy language and fuzzy logic to approach a given nonlinear continuous function with arbitrary accuracy [30], [31].

*Lemma 2* [31]: Suppose that the real continuous function  $F(\mathbf{X})$  is an arbitrary function defined on compact set  $\Omega$ . For any  $\varepsilon > 0$ , the fuzzy system  $\hat{F}(\mathbf{X}) = \boldsymbol{\theta}^{*T} \boldsymbol{\xi}(\mathbf{X})$  can be obtained, and the following condition is guaranteed:

$$\sup_{\mathbf{X} \in \Omega} |F(\mathbf{X}) - \boldsymbol{\theta}^{*T} \boldsymbol{\xi}(\mathbf{X})| \leq \varepsilon \quad (1)$$

### C. NONLINEAR TRACKING DIFFERENTIATOR

In order to estimate the uncertainties in the following section, the tracking differentiator based on improved sigmoid function (STD) is proposed in [32], and the high order STD is

formulated as follows.

$$\begin{cases} \dot{\zeta}_1 = \zeta_2 \\ \dot{\zeta}_2 = \zeta_3 \\ \vdots \\ \dot{\zeta}_{n-1} = \zeta_n \\ \dot{\zeta}_n = R^n \left[ \text{sig}(\zeta_1 - v) - \text{sig}\left(\frac{\zeta_2}{R}\right) - \dots - \text{sig}\left(\frac{\zeta_n}{R^{n-1}}\right) \right] \end{cases} \quad (2)$$

where,  $\zeta_1, \zeta_2, \dots, \zeta_n$  are state variables, and  $v, \dot{v}, \dots, v^{(n-1)}$  are the estimations of  $\zeta_1, \zeta_2, \dots, \zeta_n, v$  is the control input.  $R$  is the positive parameter to be designed.

#### D. ERROR COMPENSATION AUXILIARY SYSTEM

In the process of high-speed flight, the actuators of FAHV are usually subject to certain constraints. The normal working modes of Scramjet require a general range of fuel equivalence ratio  $\Phi$ . Considering the sensitivity of FAHV to attitude and negative impact of elastic vibration on flight vehicle, as well as the gust and turbulence will also affect the performance of the actuators, there are amplitude and rate constraints of the elevator  $\delta_e$ .

*Remark 2:* In engineering applications, fuel equivalence ratio  $\Phi$  can change at a fast rate, therefore, it generally does not affect the performance of the actuator. So in this paper, we only consider the rate constraint of elevator angular deflection  $\delta_e$ .

In order to solve the input saturation of  $\Phi$ , the problem is defined as

$$\Phi = \begin{cases} \Phi_{\max}, & \Phi_{\max} \leq \Phi_c \\ \Phi_c, & \Phi_{\min} \leq \Phi_c \leq \Phi_{\max} \\ \Phi_{\min}, & \Phi_c \leq \Phi_{\min} \end{cases} \quad (3)$$

A new auxiliary system based on error compensation is selected as

$$\dot{\vartheta}_V = -\frac{2k_V}{\pi} \text{atan}(l_V \vartheta_V) + \lambda_V (\Phi - \Phi_c) \quad (4)$$

where  $\Phi_c$  is the ideal control law to be designed with amplitude constraint,  $\Phi_{\max}$  and  $\Phi_{\min}$  are the upper and lower bounds of  $\Phi$ , respectively.  $\vartheta_V$  is the state variable of the auxiliary system,  $k_V, l_V$  and  $\lambda_V$  are parameters to be designed, and  $k_V \in R^+, l_V \in R^+, \lambda_V \in R^+$ . The schematic for amplitude limitation of fuel equivalence ratio  $\Phi$  is shown in Figure 1.

The control input constraints of  $\delta_e$  are formulated as

$$\omega_e = \begin{cases} \omega_{e\max}, & \omega_{e\max} \leq \dot{\delta}_{ec} \\ \dot{\delta}_{ec}, & \omega_{e\min} \leq \dot{\delta}_{ec} \leq \omega_{e\max} \\ \omega_{e\min}, & \dot{\delta}_{ec} \leq \omega_{e\min} \end{cases} \quad (5)$$

$$\delta_e = \begin{cases} \delta_{e\max}, & \delta_{e\max} \leq \delta_{ec} \\ \delta_{ec}, & \delta_{e\min} \leq \delta_{ec} \leq \delta_{e\max} \\ \delta_{e\min}, & \delta_{ec} \leq \delta_{e\min} \end{cases} \quad (6)$$

$\delta_{ec}$  represents the ideal control law with amplitude constraints. The change rate of  $\delta_{ec}$  can be expressed as  $\dot{\delta}_{ec}$ .

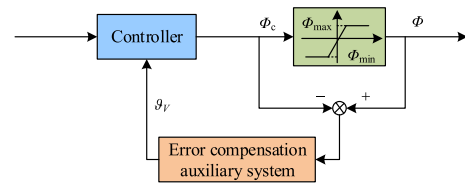


FIGURE 1. Schematic for amplitude limitation of  $\Phi$ .

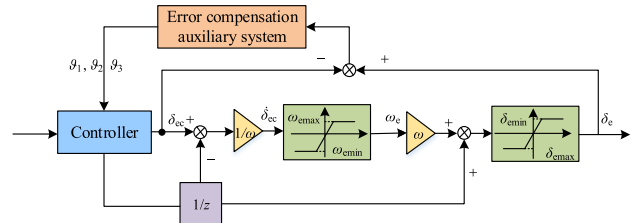


FIGURE 2. Schematic for amplitude and rate limitations of  $\delta_e$ .

$\delta_{e\max}$  and  $\delta_{e\min}$  are the upper and lower bounds of  $\delta_e$ , respectively.  $\omega_e$  represents the change rate of elevator angular deflection  $\delta_e$ .  $\omega_{e\max}$  and  $\omega_{e\min}$  are the upper and lower bounds of  $\omega_e$ . In order to deal with the amplitude and rate saturation, a high-order auxiliary system is designed by imitating the auxiliary system (7).

$$\begin{cases} \dot{\vartheta}_1 = \vartheta_2 \\ \dot{\vartheta}_2 = \vartheta_3 \\ \dot{\vartheta}_3 = -\frac{2k_1}{\pi} \text{atan}(l_1 \vartheta_1) - \frac{2k_2}{\pi} \text{atan}(l_2 \vartheta_2) - \frac{2k_3}{\pi} \text{atan}(l_3 \vartheta_3) \\ \quad + \lambda_h (\delta_e - \delta_{ec}) \end{cases} \quad (7)$$

In the high-order auxiliary system,  $\vartheta_i (i = 1, 2, 3)$  represent the state variables,  $k_i \in R^+, l_i \in R^+ (i = 1, 2, 3)$ , and  $\lambda_h \in R^+$ , they are all parameters to be designed. Considering that in the actual control system, the executable range of the actuator is also limited. This executable range is not only a rate constraint, but also an amplitude constraint during this period. Limiting the rate of elevator angular deflection is by affecting the instantaneous amplitude of the input signal in a unit time. Therefore, rate saturation can also be considered as an amplitude saturation problem in a very short time. The schematic for amplitude and rate limitations of  $\delta_e$  is shown in Figure 2.  $\omega$  represents the simulation step.

### III. DESCRIPTION OF FAHV MODEL

In 2007, Bolender and Doman in Air Force Laboratory proposed the *First Principal* model based on X-43A model and relevant theories of controller design [33], [34]. Due to the coupling phenomenon between rigid body and flexible body in the model, integrated modeling of FAHV is required. In order to facilitate the controller design, Parker weakens the coupling phenomenon and inertial coupling of rigid body and flexible body, obtained simplified model of the longitudinal

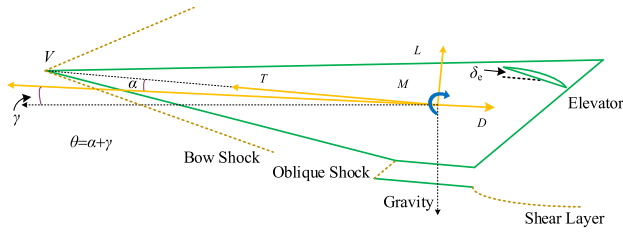


FIGURE 3. Geometry and force map of FAHV.

dynamics of FAHV [33].

$$\dot{V} = \frac{T \cos(\theta - \gamma) - D}{m} - g \sin \gamma \quad (8)$$

$$\dot{h} = V \sin \gamma \quad (9)$$

$$\dot{\gamma} = \frac{L + T \sin(\theta - \gamma)}{mV} - \frac{g}{V} \cos \gamma \quad (10)$$

$$\dot{\theta} = Q \quad (11)$$

$$\dot{Q} = \frac{M + \tilde{\psi}_1 \ddot{\eta}_1 + \tilde{\psi}_2 \ddot{\eta}_2}{I_{yy}} \quad (12)$$

$$\delta_1 \dot{\eta}_1 = -2\zeta_1 \omega_1 \dot{\eta}_1 - \omega_1^2 \eta_1 + N_1 - \tilde{\psi}_1 \frac{M}{I_{yy}} - \frac{\tilde{\psi}_1 \tilde{\psi}_2 \ddot{\eta}_2}{I_{yy}} \quad (13)$$

$$\delta_2 \dot{\eta}_2 = -2\zeta_2 \omega_2 \dot{\eta}_2 - \omega_2^2 \eta_2 + N_2 - \tilde{\psi}_2 \frac{M}{I_{yy}} - \frac{\tilde{\psi}_2 \tilde{\psi}_1 \ddot{\eta}_1}{I_{yy}} \quad (14)$$

where,

$$\begin{cases} \delta_1 = 1 + \frac{\tilde{\psi}_1}{I_{yy}} \\ \delta_2 = 1 + \frac{\tilde{\psi}_2}{I_{yy}} \\ \tilde{\psi}_1 = \int_{-L_f}^0 \hat{m}_f \xi \phi_f(\xi) d\xi \\ \tilde{\psi}_2 = \int_0^{L_a} \hat{m}_a \xi \phi_a(\xi) d\xi \end{cases}$$

$\phi_f(\cdot)$  and  $\phi_a(\cdot)$  are structural mode shapes [33]. Geometry and force map of FAHV model is shown in Figure 3.

For the rigid body state of the FAHV, the state variables are  $\{V, h, \gamma, \theta, Q\}$ . The flight velocity and flight altitude of the FAHV are expressed as  $V$  and  $h$ , respectively;  $\gamma$  represents the flight-path angle; The pitch angle and pitch rate are represented by  $\theta$  and  $Q$ , respectively;  $r$  represents the distance of the flight vehicle from the center of the earth;  $m$  is the mass of FAHV;  $I_{yy}$  represents the pitching moment of inertia of the flight vehicle; The angle of attack is defined as  $\alpha = \theta - \gamma$ . For the flexible state of the FAHV, the flexible state variables are  $\{\eta_1, \dot{\eta}_1, \eta_2, \dot{\eta}_2\}$ , and they are the first two bending modes of the fuselage.  $\zeta_1$  and  $\zeta_2$  respectively represent the damping ratio;  $\omega_1$  and  $\omega_2$  are natural frequency for flexible modes;  $N_1$  and  $N_2$  are generalized forces;  $\tilde{\psi}_1$  and  $\tilde{\psi}_2$  are the coupling coefficients of rigid body and flexible body, respectively. The lift  $L$ , the thrust  $T$ , the resistance  $D$ , the pitching moment  $M$ , and the generalized forces  $N_1$  and  $N_2$  of the vehicles are based on mechanism derivation and curve fitting, and their

expressions are as follows.

$$\begin{aligned} T &\approx C_T^{\alpha^3} \alpha^3 + C_T^{\alpha^2} \alpha^2 + C_T^{\alpha} \alpha + C_T^0 \\ D &\approx \bar{q} S \left( C_D^{\alpha^2} \alpha^2 + C_D^{\alpha} \alpha + C_D^{\delta_e^2} \delta_e^2 + C_D^{\delta_e} \delta_e + C_D^0 \right) \\ L &\approx \bar{q} S \left( C_L^{\alpha} \alpha + C_L^{\delta_e} \delta_e + C_L^0 \right) \\ M &\approx z_T T + \bar{q} S \bar{c} \left[ C_{M,\alpha}^{\alpha^2} \alpha^2 + C_{M,\alpha}^{\alpha} \alpha + C_{M,\alpha}^0 + c_e \delta_e \right] \\ N_1 &\approx N_1^{\alpha^2} \alpha^2 + N_1^{\alpha} \alpha + N_1^0 \\ N_2 &\approx N_2^{\alpha^2} \alpha^2 + N_2^{\alpha} \alpha + N_2^{\delta_e} \delta_e + N_2^0 \\ C_T^{\alpha^3} &= \beta_1(h, \bar{q}) \Phi + \beta_2(h, \bar{q}) \\ C_T^{\alpha^2} &= \beta_3(h, \bar{q}) \Phi + \beta_4(h, \bar{q}) \\ C_T^{\alpha} &= \beta_5(h, \bar{q}) \Phi + \beta_6(h, \bar{q}) \\ C_T^0 &= \beta_7(h, \bar{q}) \Phi + \beta_8(h, \bar{q}) \\ \bar{q} &= \frac{1}{2} \bar{\rho} V^2, \bar{\rho} = \bar{\rho}_0 \exp\left(\frac{h_0 - h}{h_s}\right) \end{aligned}$$

The inputs of control system are fuel equivalence ratio  $\Phi$  and elevator angular deflection  $\delta_e$ . The aerodynamic pressure of the vehicle is  $\bar{q}$  and the average air density is  $\bar{\rho}$ . The reference area and the average aerodynamic chord length of flight vehicle are  $S$  and  $\bar{c}$ , respectively. For other parameters in the expression, the reader can refer to [33].

*Remark 3:* In the following, since the state variables of rigid body are measurable, we use five rigid state variables for the controller design. In reality, the flexible state cannot be accurately measured, so we take the flexible state as the system uncertainties and deal it with the fuzzy approximator in the controller.

*Remark 4:* Under the assumption that the FAHV model is unknown, its control objective is to ensure that the velocity  $V$  and altitude  $h$  can robustly track the respective reference inputs by designing appropriate control laws.

#### IV. CONTROLLER DESIGN

In order to facilitate the design of the control laws, the FAHV model is decomposed into the velocity subsystem (such as Eq.(8)) and the altitude subsystem (Eqs.(9)~(12)), and the control laws are designed separately.

##### A. CONTROLLER DESIGN OF VELOCITY SUBSYSTEM

The control objective of the velocity subsystem is to design a appropriate control law for  $\Phi$  to achieve robust tracking of velocity  $V$  to its reference input  $V_{ref}$  based on non-affine models of FAHV.

According to the research conclusions of [33] and [34], the velocity subsystem can be rewritten into a non-affine form.

$$\dot{V} = G_V(V, \Phi) \quad (15)$$

where  $G_V(V, \Phi)$  is a completely unknown nonlinear function.

Firstly, the following assumption is given to the control system.

*Assumption 1:* For any  $(V, \Phi) \in \Omega_V \times R$ , the following inequality is established:

$$\frac{\partial G_V(V, \Phi)}{\partial \Phi} > 0 \tag{16}$$

where,  $\Omega_V$  is a controllable area.

*Remark 5:* According to the research data given in [33], based on the range of FAHV rigid body state, assumption 1 is valid.

Velocity tracking error is defined as

$$\tilde{V} = V - V_{ref} \tag{17}$$

Taking time derivative along (17)

$$\dot{\tilde{V}} = \dot{V} - \dot{V}_{ref} \tag{18}$$

Substituting Eq. (15) into Eq. (18)

$$\dot{\tilde{V}} = \dot{V} - \dot{V}_{ref} = \lambda_V \Phi + g_V(V, \Phi) - \dot{V}_{ref} \tag{19}$$

where  $\lambda_V \in R^+$  is the parameter to be designed and  $g_V(V, \Phi) = G_V(V, \Phi) - \lambda_V \Phi$  is a completely unknown nonlinear function.

The control law of velocity subsystem is designed as

$$\Phi = \lambda_V^{-1} (\Phi_0 - \Phi_1) \tag{20}$$

where,  $\Phi_0 = -\lambda_{V,1} \tilde{V} - \lambda_{V,2} \int_0^t \tilde{V} d\tau + \dot{V}_{ref}$ ,  $\lambda_{V,1} \in R^+$  and  $\lambda_{V,2} \in R^+$  are the parameters to be designed. In addition, the fuzzy control law  $\Phi_1$  is designed to offset the influence of the uncertainty term  $g_V(V, \Phi)$ .

According to the uniqueness theorem of implicit function introduced in the previous section, there is  $\Phi_1^* \in R$ , which satisfies

$$G_1(V, \Phi_0, \Phi_1^*) \triangleq g_V(V, \lambda_V^{-1} (\Phi_0 - \Phi_1^*)) - \Phi_1^* = 0 \tag{21}$$

Then we can get the following theorem 1

*Theorem 1:* Define

$$\lambda_V > \frac{1}{2} \frac{\partial G_V(V, \Phi)}{\partial \Phi} \tag{22}$$

Then there are a controllable area  $\Omega_V \subset R$  and a unique  $\Phi_1^*(V, \Phi_0)$ , for any  $(V, \Phi_0) \in \Omega_V \times R$ ,  $\Phi_1^*(V, \Phi_0)$  satisfies (23).

*Proof:* According to the research [29] and [35], if the following inequality holds, it can get  $\Phi_1^*$  to exist.

$$\left| \frac{\partial g_V(V, \Phi)}{\partial \Phi_1^*} \right| < 1 \tag{23}$$

Combining  $g_V(V, \Phi) = G_V(V, \Phi) - \lambda_V \Phi$  and Eqs. (16), (18), (22), we can get

$$\begin{aligned} \left| \frac{\partial g_V(V, \Phi)}{\partial \Phi_1^*} \right| &= \left| \frac{\partial [G_V(V, \Phi) - \lambda_V \Phi]}{\partial \Phi_1^*} \right| \\ &= \left| \frac{\partial [G_V(V, \Phi) - \lambda_V \Phi]}{\partial \Phi} \frac{\partial \Phi}{\partial \Phi_1^*} \right| \\ &= \left| \left[ \frac{\partial G_V(V, \Phi)}{\partial \Phi} - \lambda_V \right] \frac{1}{\lambda_V} \right| \\ &= \left| \frac{1}{\lambda_V} \frac{\partial G_V(V, \Phi)}{\partial \Phi} - 1 \right| < 1 \end{aligned} \tag{24}$$

So we can get  $\Phi_1^*$  to exist, further we can get

$$\begin{aligned} \frac{\partial}{\partial \Phi_1^*} G_1(V, \Phi_0, \Phi_1^*) &= \frac{\partial}{\partial \Phi_1^*} [g_V(V, \Phi^*) - \Phi_1^*] \\ &= \frac{\partial}{\partial \Phi^*} [G_V(V, \Phi^*) - \lambda_V \Phi^*] \frac{\partial \Phi^*}{\partial \Phi_1^*} - 1 \\ &= \left[ \frac{\partial}{\partial \Phi^*} G_V(V, \Phi^*) - \lambda_V \right] \left( -\frac{1}{\lambda_V} \right) - 1 \\ &= -\frac{1}{\lambda_V} \frac{\partial G_V(V, \Phi^*)}{\partial \Phi^*} \end{aligned} \tag{25}$$

where  $\Phi^* = \lambda_V^{-1} (\Phi_0 - \Phi_1^*)$ . It can be obtained from Eqs. (16) and (22) that  $\partial G_1(V, \Phi_0, \Phi_1^*) / (\partial \Phi_1^*)$  is non-singular, therefore, theorem 1 is established.

At the same time, theorem 1 also shows that for any  $(V, \Phi_0) \in \Omega_V \times R$ ,  $\Phi_0$  can be regarded as a function of  $V$  and  $\Phi_0$ , so that according to  $\Phi = \lambda_V^{-1} (\Phi_0 - \Phi_1)$ ,  $\Phi$  can also be regarded as a function of  $V$  and  $\Phi_0$ . Then,  $g_V(V, \Phi) = G_V(V, \Phi) - \lambda_V \Phi$  can also be regarded as a function of  $V$  and  $\Phi_0$ .

Assuming that the function  $g_V$  is an unknown function, the fuzzy system is introduced to approximate the function  $g_V$ . The input of the fuzzy system is  $X_1 = [V, \Phi_0]^T \in R^2$ , the ideal weight coefficient parameter vector is selected as  $\theta_1^* = [\theta_{11}^*, \theta_{12}^*, \dots, \theta_{1w_1}^*]^T \in R^{w_1}$ , Gauss basis function is selected as membership function, and the vector of the fuzzy basis function is  $\xi_1(X_1) = [\xi_{11}(X_1), \xi_{12}(X_1), \dots, \xi_{1w_1}(X_1)]^T \in R^{w_1}$ .  $\varepsilon_1 \in R$  represents the approximation error and  $\varepsilon_{1M} \in R^+$  represents the upper bound of the approximation error.

Fuzzy approximator can be expressed as

$$g_V(V, \Phi) = \theta_1^{*T} \xi_1(X_1) + \varepsilon_1, |\varepsilon_1| \leq \varepsilon_{1M} \tag{26}$$

Define  $\varphi_V = \|\theta_1^*\|^2$ , design  $\Phi_1$  is

$$\Phi_1 = -\frac{1}{2} \tilde{V} \hat{\varphi}_V \xi_1^T(X_1) \xi_1(X_1) \tag{27}$$

where,  $\hat{\varphi}_V$  is the estimate of  $\varphi_V$  and its adaptive law is designed as

$$\dot{\hat{\varphi}}_V = \frac{\kappa_V}{2} \tilde{V}^2 \xi_1^T(X_1) \xi_1(X_1) - 2\hat{\varphi}_V \tag{28}$$

where  $\kappa_V \in R^+$  is the parameter to be designed.

Introducing the error compensation auxiliary system proposed in previous section.

Improve the velocity tracking error as

$$z_V = \tilde{V} - \vartheta_V \tag{29}$$

Taking time derivative along (29) and combine the Eqs. (19) and (7), we can get

$$\begin{aligned} \dot{z}_V &= \dot{\tilde{V}} - \dot{\vartheta}_V \\ &= \lambda_V \Phi + g_V(V, \Phi) - \dot{V}_{ref} \\ &\quad - \left[ -\frac{2\kappa_V}{\pi} \text{atan}(l_V \vartheta_V) + \lambda_V (\Phi - \Phi_c) \right] \\ &= \lambda_V \Phi_c + g_V(V, \Phi) - \dot{V}_{ref} + \frac{2\kappa_V}{\pi} \text{atan}(l_V \vartheta_V) \end{aligned} \tag{30}$$

The ideal control law  $\Phi_c$  in the case of input constraint is redesigned as

$$\Phi_c = \lambda_V^{-1} (\Phi_0 - \Phi_1) \quad (31)$$

where  $\Phi_0 = -\lambda_{V,1} z_V - \lambda_{V,2} \int_0^t z_V d\tau + \dot{V}_{\text{ref}} - \frac{2\kappa_V}{\pi} \text{atan}(l_V \vartheta_V)$  and  $\Phi_1$  is modified to

$$\Phi_1 = \frac{1}{2} z_V \hat{\varphi}_V \xi_1^T(\mathbf{X}_1) \xi_1(\mathbf{X}_1) \quad (32)$$

Then, the adaptive law of  $\hat{\varphi}_V$  is designed as

$$\dot{\hat{\varphi}}_V = \frac{\kappa_V}{2} z_V^2 \xi_1^T(\mathbf{X}_1) \xi_1(\mathbf{X}_1) - 2\hat{\varphi}_V \quad (33)$$

$\kappa_V \in R^+$  is the parameter to be designed.

*Remark 6:* [13] and [36] directly adjust the elements of the weight vector  $\theta$  online. Compared with [13], the fuzzy control law adopted in this paper does not need a large number of recursive processes in the back-stepping control, and the control law adopts norm estimation approach, which only need one online learning parameter and greatly reduces the computational load of the system.

## B. CONTROLLER DESIGN OF ALTITUDE SUBSYSTEM

The control objective of the altitude subsystem is to design a appropriate control law based on the non-affine models for  $\delta_e$  to achieve robust tracking of  $h$  to its reference input  $h_{\text{ref}}$ .

Define the altitude tracking error as

$$\tilde{h} = h - h_{\text{ref}} \quad (34)$$

Through feedback transformation, the control objective of the altitude subsystem is transformed into  $\gamma \rightarrow \gamma_d$  by selecting the appropriate feedback control input  $\delta_e$  [37].

The reference trajectory of  $\gamma$  is chosen as

$$\gamma_d = \arcsin\left(\frac{-k_h \tilde{h} + \dot{h}_{\text{ref}}}{V}\right) \quad (35)$$

where,  $k_h \in R^+$  is the parameter to be designed.

First, give a reasonable assumption for the altitude subsystem.

*Assumption 2:* For any  $(\boldsymbol{\psi}, \delta_e) \in \Omega_{\boldsymbol{\psi}} \times R$ , the following inequality is established.

$$\begin{cases} \frac{\partial G_{h1}(\psi_1, \psi_2)}{\partial \psi_2} > 0 \\ \frac{\partial G_{h3}(\boldsymbol{\psi}, \delta_e)}{\partial \delta_e} > 0 \end{cases} \quad (36)$$

where  $\Omega_{\boldsymbol{\psi}}$  is a controllable area.

*Remark 7:* According to [30] and FAHV's ranges of rigid body state, it can be known that Assumption 2 are valid.

By defining  $\psi_1 = \gamma$ ,  $\psi_2 = \theta$  and  $\psi_3 = Q$ , the remaining part of FAHV altitude subsystem (Eqs.(10)~(12)) can be expressed as non-affine forms as follows.

$$\begin{cases} \dot{\psi}_1 = G_{h1}(\psi_1, \psi_2) \\ \dot{\psi}_2 = \psi_3 \\ \dot{\psi}_3 = G_{h3}(\boldsymbol{\psi}, \delta_e) \end{cases} \quad (37)$$

where,  $G_{h1}(\psi_1, \psi_2)$  and  $G_{h3}(\boldsymbol{\psi}, \delta_e)$  are continuous unknown functions,  $\boldsymbol{\psi} = [\psi_1, \psi_2, \psi_3]^T$ .

Define  $\chi_1 = \psi_1 = \gamma$ ,  $\chi_2 = \dot{\chi}_1 = G_{h1}(\psi_1, \psi_2)$  and transform Eq. (37). According to Eq. (37), the time derivative of  $\chi_2$  is derived as

$$\begin{aligned} \dot{\chi}_2 &= \frac{\partial G_{h1}(\psi_1, \psi_2)}{\partial \psi_1} \dot{\psi}_1 + \frac{\partial G_{h1}(\psi_1, \psi_2)}{\partial \psi_2} \dot{\psi}_2 \\ &= \frac{\partial G_{h1}(\psi_1, \psi_2)}{\partial \psi_1} G_{h1}(\psi_1, \psi_2) + \frac{\partial G_{h1}(\psi_1, \psi_2)}{\partial \psi_2} \psi_3 \\ &\triangleq g_{h1}(\boldsymbol{\psi}) \end{aligned} \quad (38)$$

Then, define  $\chi_3 = \dot{\chi}_2 = g_{h1}(\boldsymbol{\psi})$ . Applying (37), the time derivative of  $\chi_3$  is derived as

$$\begin{aligned} \dot{\chi}_3 &= \frac{\partial g_{h1}(\boldsymbol{\psi})}{\partial \psi_1} \dot{\psi}_1 + \frac{\partial g_{h1}(\boldsymbol{\psi})}{\partial \psi_2} \dot{\psi}_2 + \frac{\partial g_{h1}(\boldsymbol{\psi})}{\partial \psi_3} \dot{\psi}_3 \\ &= \frac{\partial g_{h1}(\boldsymbol{\psi})}{\partial \psi_1} G_{h1}(\psi_1, \psi_2) + \frac{\partial g_{h1}(\boldsymbol{\psi})}{\partial \psi_2} \psi_3 \\ &\quad + \frac{\partial g_{h1}(\boldsymbol{\psi})}{\partial \psi_3} G_{h3}(\boldsymbol{\psi}, \delta_e) \\ &\triangleq g_{h2}(\boldsymbol{\psi}, \delta_e) \end{aligned} \quad (39)$$

After two model transformations, (37) is written as non-affine pure feedback forms as follows

$$\begin{cases} \dot{\chi}_1 = \chi_2 \\ \dot{\chi}_2 = \chi_3 \\ \dot{\chi}_3 = g_{h2}(\boldsymbol{\psi}, \delta_e) \end{cases} \quad (40)$$

where  $g_{h2}(\boldsymbol{\psi}, \delta_e)$  is a completely unknown nonlinear function.

*Remark 8:* According to Eqs. (36)~(39), it can be obtained.

$$\begin{aligned} \frac{\partial g_{h2}(\boldsymbol{\psi}, \delta_e)}{\partial \delta_e} &= \frac{\partial g_{h1}(\boldsymbol{\psi})}{\partial \psi_3} \frac{\partial G_{h3}(\boldsymbol{\psi}, \delta_e)}{\partial \delta_e} \\ &= \frac{\partial G_{h1}(\psi_1, \psi_2)}{\partial \psi_2} \frac{\partial G_{h3}(\boldsymbol{\psi}, \delta_e)}{\partial \delta_e} > 0 \end{aligned} \quad (41)$$

*Remark 9:* The forms of Eq. (37) are equivalent to the forms of Eq. (40). Compared with Eq. (37), Eq. (40) is a pure feedback model with a non-affine formulation containing only one unknown function  $g_{h2}(\boldsymbol{\psi}, \delta_e)$ .

The tracking error and error function of flight-path tracking error are defined as  $e$  and  $E$ , respectively.

$$\begin{cases} e = \gamma - \gamma_d = \chi_1 - \gamma_d \\ E = \left(\frac{d}{dt} + \bar{h}\right)^3 \int_0^t e d\tau \\ = \ddot{e} + 3\bar{h}\dot{e} + 3\bar{h}^2 e + \bar{h}^3 \int_0^t e d\tau \end{cases} \quad (42)$$

where  $\bar{h} \in R^+$  is the parameter to be designed. Since  $(s + \bar{h})^3$  is a Hurwitz polynomial. If  $E$  is bounded,  $e$  is also bounded.

According to (40) and (42), we obtain

$$\begin{cases} \dot{e} = \dot{\chi}_1 - \dot{\gamma}_d = \chi_2 - \dot{\gamma}_d \\ \ddot{e} = \dot{\chi}_2 - \ddot{\gamma}_d = \chi_3 - \ddot{\gamma}_d \\ e = \dot{\chi}_3 - \dot{\gamma}_d = \lambda_h \delta_e + F_h(\boldsymbol{\psi}, \delta_e) - \dot{\gamma}_d \end{cases} \quad (43)$$

where,  $F_h(\boldsymbol{\psi}, \delta_e) = -\lambda_h \delta_e + g_{h2}(\boldsymbol{\psi}, \delta_e)$  is a continuously differentiable nonlinear unknown function and  $\lambda_h \in R^+$  is a parameter to be designed.

Because  $\chi_2 = \dot{\gamma}$  and  $\chi_3 = \dot{\gamma}$  are unknown, in order to obtain the estimations of  $\chi_2$  and  $\chi_3$ , the fourth-order STD proposed in the previous section is introduced, and  $\gamma$  is used as the input signal of the fourth-order STD. Similarly,  $\gamma_d$  is used as the input signal of the fourth-order STD, and the estimations  $\hat{\gamma}_d$ ,  $\hat{\dot{\gamma}}_d$ , and  $\hat{\ddot{\gamma}}_d$  of  $\gamma_d$ ,  $\dot{\gamma}_d$  and  $\ddot{\gamma}_d$  are also obtained.

Therefore, the estimations of the first three derivatives of  $e$  can be expressed as

$$\begin{cases} \dot{\hat{e}} = \hat{\chi}_2 - \hat{\dot{\gamma}}_d \\ \ddot{\hat{e}} = \hat{\chi}_3 - \hat{\ddot{\gamma}}_d \\ \hat{e} = \tau_h \delta_e + F_h(\boldsymbol{\psi}, \delta_e) - \hat{\gamma}_d \end{cases} \quad (44)$$

From (42) and (44), we obtain the estimation of  $E$ .

$$\dot{\hat{E}} = \lambda_h \delta_e + F_h(\boldsymbol{\psi}, \delta_e) - \hat{\gamma}_d + 3\hat{h}\ddot{\hat{e}} + 3\hat{h}^2\dot{\hat{e}} + \hat{h}^3\hat{e}$$

Define

$$\delta_{e0} = -\tau_h \hat{E} + \hat{\gamma}_d - 3\hat{h}\ddot{\hat{e}} - 3\hat{h}^2\dot{\hat{e}} - \hat{h}^3\hat{e}$$

where,  $\tau_h \in R^+$ .

Control law of altitude subsystem is designed as

$$\delta_e = \lambda_h^{-1} (\delta_{e0} - \delta_{e1}) \quad (45)$$

where  $\delta_{e1}$  is the fuzzy control law to be designed to counteract the influence of the uncertain term  $F_h(\boldsymbol{\psi}, \delta_e)$ .

According to the uniqueness theorem of implicit function above, there must be a  $\delta_{e1}^*$  such that the Eq.(46) holds.

$$G_2(\boldsymbol{\psi}, \delta_{e0}, \delta_{e1}^*) F_h(\boldsymbol{\psi}, \lambda_h^{-1} (\delta_{e0} - \delta_{e1}^*)) - \delta_{e1}^* = 0 \quad (46)$$

Give the following theorem 2

*Theorem 2:* Define

$$\lambda_h > \frac{1}{2} \frac{\partial g_{h2}(\boldsymbol{\psi}, \delta_e)}{\partial \delta_e} \quad (47)$$

There are a controllable area  $\Omega_{\boldsymbol{\psi}} \subset R^3$  and a unique  $\delta_{e1}^*(\boldsymbol{\psi}, \delta_e)$ , for any  $(\boldsymbol{\psi}, \delta_e) \in \Omega_{\boldsymbol{\psi}} \times R$ ,  $\delta_{e1}^*(\boldsymbol{\psi}, \delta_e)$  satisfies (47).

*Proof:* According to the research [33] and [34], if the following inequality holds, it can get  $\delta_{e1}^*$  to exist.

$$\left| \frac{\partial F_h(\boldsymbol{\psi}, \delta_e)}{\partial \delta_{e1}^*} \right| < 1 \quad (48)$$

According to Eqs. (41), (45) and (47), the equation (49) holds.

$$\begin{aligned} \left| \frac{\partial F_h(\boldsymbol{\psi}, \delta_e)}{\partial \delta_{e1}^*} \right| &= \left| \frac{\partial [g_{h2}(\boldsymbol{\psi}, \delta_e) - \lambda_h \delta_e]}{\partial \delta_{e1}^*} \right| \\ &= \left| \frac{\partial [g_{h2}(\boldsymbol{\psi}, \delta_e) - \lambda_h \delta_e]}{\partial \delta_e} \frac{\partial \delta_e}{\partial \delta_{e1}^*} \right| \\ &= \left| \left[ \frac{\partial g_{h2}(\boldsymbol{\psi}, \delta_e)}{\partial \delta_e} - \lambda_h \right] \frac{1}{\lambda_h} \right| \\ &= \left| \frac{1}{\lambda_h} \frac{\partial g_{h2}(\boldsymbol{\psi}, \delta_e)}{\partial \delta_e} - 1 \right| < 1 \end{aligned} \quad (49)$$

Therefore,  $\delta_{e1}^*$  exists.

Because

$$\begin{aligned} \frac{\partial}{\partial \delta_{e1}^*} G_2(\boldsymbol{\psi}, \delta_{e0}, \delta_{e1}^*) &= \frac{\partial}{\partial \delta_{e1}^*} [F_h(\boldsymbol{\psi}, \delta_e^*) - \delta_{e1}^*] \\ &= \frac{\partial}{\partial \delta_{e1}^*} [g_{h2}(\boldsymbol{\psi}, \delta_e^*) - \lambda_h \delta_e^*] - 1 \\ &= \frac{\partial}{\partial \delta_e^*} [g_{h2}(\boldsymbol{\psi}, \delta_e^*) - \lambda_h \delta_e^*] \frac{\partial \delta_e^*}{\partial \delta_{e1}^*} - 1 \\ &= \left[ \frac{\partial g_{h2}(\boldsymbol{\psi}, \delta_e^*)}{\partial \delta_e^*} - \lambda_h \right] \left( -\frac{1}{\lambda_h} \right) - 1 \\ &= -\frac{1}{\lambda_h} \frac{\partial g_{h2}(\boldsymbol{\psi}, \delta_e^*)}{\partial \delta_e^*} \end{aligned} \quad (50)$$

where,  $\delta_e^* = \lambda_h^{-1} (\delta_{e0} - \delta_{e1}^*)$ . We can see that  $\partial G_2(\boldsymbol{\psi}, \delta_{e0}, \delta_{e1}^*) / (\partial \delta_{e1}^*)$  is nonsingular, so we can get theorem 3.

According to Theorem 3, we can consider  $\delta_e$  as a function of  $\boldsymbol{\psi}$  and  $\delta_{e0}$ , and regard  $F_h(\boldsymbol{\psi}, \delta_e)$  as a function of  $\boldsymbol{\psi}$  and  $\delta_{e0}$ .

Next, a fuzzy approximator is introduced into the altitude subsystem to approximate  $F_h(\boldsymbol{\psi}, \delta_e)$ .

Define the input of the fuzzy system as  $X_2 = [\boldsymbol{\psi}^T, \delta_{e0}]^T \in R^4$ , the ideal weight coefficient parameter vector is selected as  $\boldsymbol{\theta}_2^* = [\theta_{21}^*, \theta_{22}^*, \dots, \theta_{2w_2}^*]^T \in R^{w_2}$ , the vector of the fuzzy basis function is  $\boldsymbol{\xi}_2(X_2) = [\xi_{21}(X_2), \xi_{22}(X_2), \dots, \xi_{2w_2}(X_2)]^T \in R^{w_2}$ .  $\varepsilon_2 \in R$  represents the approximation error and  $\varepsilon_{2M} \in R^+$  represents the upper bound of the approximation error. Fuzzy approximator can be expressed as

$$F_h(\boldsymbol{\psi}, \delta_e) = \boldsymbol{\theta}_2^{*T} \boldsymbol{\xi}_2(X_2) + \varepsilon_2, |\varepsilon_2| \leq \varepsilon_{2M} \quad (51)$$

Design  $\delta_{e1}$  as

$$\delta_{e1} = \frac{1}{2} \hat{E} \hat{\varphi}_h \boldsymbol{\xi}_2^T(X_2) \boldsymbol{\xi}_2(X_2) \quad (52)$$

where,  $\varphi_h = \|\boldsymbol{\theta}_2^*\|^2$  and  $\hat{\varphi}_h$  are the estimated values of  $\varphi_h$ , and the design adaptive law is

$$\dot{\hat{\varphi}}_h = \frac{\kappa_h}{2} \hat{E}^2 \boldsymbol{\xi}_2^T(X_2) \boldsymbol{\xi}_2(X_2) - 2\hat{\varphi}_h \quad (53)$$

where,  $\kappa_h \in R^+$  is the parameter to be designed.

In order to deal with the saturation problem of  $\delta_e$ , the high-order error compensation auxiliary system proposed in (7) is introduced to correct the flight-path tracking error  $e$  and the error function  $E$ .

$$\begin{cases} z_\gamma = e - \vartheta_1 \\ z_E = \left( \frac{d}{dt} + \hat{h} \right)^3 \int_0^t z_\gamma(\tau) d\tau \end{cases} \quad (54)$$

Therefore, if  $z_E$  is bounded, we can get  $z_\gamma$  is bounded.

The first three derivatives of  $z_\gamma$  can be expressed as

$$\begin{cases} \dot{z}_\gamma = \dot{e} - \dot{\vartheta}_1 = \chi_2 - \dot{\gamma}_d - \vartheta_2 \\ \ddot{z}_\gamma = \dot{\chi}_2 - \ddot{\gamma}_d - \dot{\vartheta}_2 = \chi_3 - \ddot{\gamma}_d - \vartheta_3 \\ z_\gamma = \dot{\chi}_3 - \gamma_d - \dot{\vartheta}_3 = \lambda_h \delta_e + F_h(\boldsymbol{\psi}, \delta_e) - \gamma_d \\ \quad + \frac{2k_1}{\pi} \text{atan}(l_1 \vartheta_1) + \frac{2k_2}{\pi} \text{atan}(l_2 \vartheta_2) \\ \quad + \frac{2k_3}{\pi} \text{atan}(l_3 \vartheta_3) - \lambda_h (\delta_e - \delta_{ec}) \\ = \lambda_h \delta_e + F_h(\boldsymbol{\psi}, \delta_e) - \gamma_d + \frac{2k_1}{\pi} \text{atan}(l_1 \vartheta_1) \\ \quad + \frac{2k_2}{\pi} \text{atan}(l_2 \vartheta_2) + \frac{2k_3}{\pi} \text{atan}(l_3 \vartheta_3) \end{cases} \quad (55)$$

Taking time derivative along (54)

$$\begin{aligned} \dot{z}_E &= z_\gamma + 3\dot{h}\ddot{z}_\gamma + 3\dot{h}^2\dot{z}_\gamma + \dot{h}^3z_\gamma \\ &= \lambda_h \delta_{ec} + F_h(\boldsymbol{\psi}, \delta_e) - \gamma_d + \frac{2k_1}{\pi} \text{atan}(l_1 \vartheta_1) \\ &\quad + \frac{2k_2}{\pi} \text{atan}(l_2 \vartheta_2) + \frac{2k_3}{\pi} \text{atan}(l_3 \vartheta_3) \\ &\quad + 3\dot{h}\ddot{z}_\gamma + 3\dot{h}^2\dot{z}_\gamma + \dot{h}^3z_\gamma \end{aligned} \quad (56)$$

Estimating unknown state variables by using fourth-order STD, the estimations of  $\chi_2$  and  $\chi_3$  are  $\hat{\chi}_2$  and  $\hat{\chi}_3$ . The first three derivatives of  $\gamma_d$  are denoted by  $\hat{\gamma}_d$ ,  $\dot{\hat{\gamma}}_d$  and  $\ddot{\hat{\gamma}}_d$ , respectively.

$$\begin{cases} \dot{\hat{z}}_\gamma = \dot{e} - \dot{\vartheta}_1 = \hat{\chi}_2 - \dot{\hat{\gamma}}_d - \vartheta_2 \\ \ddot{\hat{z}}_\gamma = \dot{\hat{\chi}}_2 - \ddot{\hat{\gamma}}_d - \dot{\vartheta}_2 = \hat{\chi}_3 - \ddot{\hat{\gamma}}_d - \vartheta_3 \\ \hat{z}_\gamma = \lambda_h \delta_{ec} + F_h(\boldsymbol{\psi}, \delta_e) - \hat{\gamma}_d + \frac{2k_1}{\pi} \text{atan}(l_1 \vartheta_1) \\ \quad + \frac{2k_2}{\pi} \text{atan}(l_2 \vartheta_2) + \frac{2k_3}{\pi} \text{atan}(l_3 \vartheta_3) \end{cases} \quad (57)$$

$$\begin{aligned} \dot{\hat{z}}_E &= \lambda_h \delta_{ec} + F_h(\boldsymbol{\psi}, \delta_e) - \hat{\gamma}_d + \frac{2k_1}{\pi} \text{atan}(l_1 \vartheta_1) \\ &\quad + \frac{2k_2}{\pi} \text{atan}(l_2 \vartheta_2) + \frac{2k_3}{\pi} \text{atan}(l_3 \vartheta_3) \\ &\quad + 3\dot{h}\ddot{\hat{z}}_\gamma + 3\dot{h}^2\dot{\hat{z}}_\gamma + \dot{h}^3\hat{z}_\gamma \end{aligned} \quad (58)$$

In the constrained case, redesign the ideal control law  $\delta_{ec}$  as

$$\delta_{ec} = \lambda_h^{-1} (\delta_{e0} - \delta_{e1}) \quad (59)$$

where,

$$\begin{aligned} \delta_{e0} &= -\tau_h \hat{z}_E + \ddot{\hat{\gamma}}_d - 3\dot{h}\ddot{\hat{z}}_\gamma - 3\dot{h}^2\dot{\hat{z}}_\gamma - \dot{h}^3\hat{z}_\gamma \\ &\quad - \frac{2k_1}{\pi} \text{atan}(l_1 \vartheta_1) - \frac{2k_2}{\pi} \text{atan}(l_2 \vartheta_2) \\ &\quad - \frac{2k_3}{\pi} \text{atan}(l_3 \vartheta_3) \end{aligned} \quad (60)$$

$\delta_{e1}$  is the fuzzy control law to be designed to offset the uncertainty term  $F_h(\boldsymbol{\psi}, \delta_e)$  in the case of input saturation,  $\tau_h \in R^+$  is a parameter to be designed, and  $\delta_{e1}$  is redesigned as

$$\delta_{e1} = \frac{1}{2} \hat{z}_E \hat{\varphi}_h \boldsymbol{\xi}_2^T(\mathbf{X}_2) \boldsymbol{\xi}_2(\mathbf{X}_2) \quad (61)$$

The adaptive law is redesigned as

$$\dot{\hat{\varphi}}_h = \frac{\kappa_h}{2} \hat{z}_E^2 \boldsymbol{\xi}_2^T(\mathbf{X}_2) \boldsymbol{\xi}_2(\mathbf{X}_2) - 2\hat{\varphi}_h \quad (62)$$

$\kappa_h \in R^+$  is the parameter to be designed.

## V. STABILITY ANALYSIS

### A. STABILITY ANALYSIS OF VELOCITY SUBSYSTEM

*Theorem 3:* Consider the closed-loop velocity subsystem of FAHV(15), consisting of control law (31), adaptive law (33), and the amplitude saturation error compensation auxiliary system (7) under the premise of Theorem 1, then the closed-loop control system is semiglobally uniformly ultimately bounded.

*Proof:* Define estimation error

$$\tilde{\varphi}_V = \hat{\varphi}_V - \varphi_V \quad (63)$$

Substituting Eqs. (26), (31), and (32) into Eq. (32)

$$\begin{aligned} \dot{z}_V &= \Phi_0 - \Phi_1 + \boldsymbol{\theta}_1^{*T} \boldsymbol{\xi}_1(\mathbf{X}_1) + \varepsilon_1 - \dot{V}_{\text{ref}} + \frac{2\kappa_V}{\pi} \text{atan}(l_V \vartheta_V) \\ &= -\lambda_{V,1} z_V - \lambda_{V,2} \int_0^t z_V d\tau - \frac{1}{2} z_V \hat{\varphi}_1 \boldsymbol{\xi}_1^T(\mathbf{X}_1) \boldsymbol{\xi}_1(\mathbf{X}_1) \\ &\quad + \boldsymbol{\theta}_1^{*T} \boldsymbol{\xi}_1(\mathbf{X}_1) + \varepsilon_1 \end{aligned} \quad (64)$$

Select the Lyapunov function as

$$L_V = \frac{1}{2} z_V^2 + \frac{1}{2} \lambda_{V,2} \left( \int_0^t z_V d\tau \right)^2 + \frac{\tilde{\varphi}_V^2}{2\kappa_V} \quad (65)$$

Differentiating (65) with respect to time and substituting (33) and (64) to get

$$\begin{aligned} \dot{L}_V &= z_V \dot{z}_V + \lambda_{V,2} z_V \int_0^t z_V d\tau + \frac{\tilde{\varphi}_V \dot{\tilde{\varphi}}_V}{\kappa_V} \\ &= z_V \left[ -\lambda_{V,1} z_V - \lambda_{V,2} \int_0^t z_V d\tau - \frac{1}{2} z_V \hat{\varphi}_V \boldsymbol{\xi}_1^T(\mathbf{X}_1) \boldsymbol{\xi}_1(\mathbf{X}_1) \right. \\ &\quad \left. + \boldsymbol{\theta}_1^{*T} \boldsymbol{\xi}_1(\mathbf{X}_1) + \varepsilon_1 \right] \\ &\quad + \lambda_{V,2} z_V \int_0^t z_V d\tau + \frac{\tilde{\varphi}_V}{\kappa_V} \left[ \frac{\kappa_V}{2} z_V^2 \boldsymbol{\xi}_1^T(\mathbf{X}_1) \boldsymbol{\xi}_1(\mathbf{X}_1) - 2\dot{\tilde{\varphi}}_V \right] \\ &= -\lambda_{V,1} z_V^2 - \frac{1}{2} z_V^2 \varphi_V \boldsymbol{\xi}_1^T(\mathbf{X}_1) \boldsymbol{\xi}_1(\mathbf{X}_1) + z_V \boldsymbol{\theta}_1^{*T} \boldsymbol{\xi}_1(\mathbf{X}_1) \\ &\quad + z_V \varepsilon_1 - \frac{2\tilde{\varphi}_V \dot{\tilde{\varphi}}_V}{\kappa_V} \end{aligned} \quad (66)$$

Owing to

$$\begin{aligned} z_V \varepsilon_1 &\leq \frac{z_V^2}{4} + \varepsilon_{1M}^2 \\ 2\tilde{\varphi}_V \dot{\tilde{\varphi}}_V &\geq \dot{\tilde{\varphi}}_V^2 - \varphi_V^2 \\ z_V \boldsymbol{\theta}_1^{*T} \boldsymbol{\xi}_1(\mathbf{X}_1) &\leq \frac{z_V^2}{2} \left\| \boldsymbol{\theta}_1^{*T} \boldsymbol{\xi}_1(\mathbf{X}_1) \right\|^2 + \frac{1}{2} \\ &= \frac{z_V^2}{2} \left\| \boldsymbol{\theta}_1^* \right\|^2 \left\| \boldsymbol{\xi}_1(\mathbf{X}_1) \right\|^2 + \frac{1}{2} \\ &= \frac{z_V^2}{2} \varphi_V \boldsymbol{\xi}_1^T(\mathbf{X}_1) \boldsymbol{\xi}_1(\mathbf{X}_1) + \frac{1}{2} \end{aligned}$$



Eq. (66) is converted to

$$\dot{L}_V \leq - \left( \lambda_{V,1} - \frac{1}{4} \right) z_V^2 - \frac{\tilde{\varphi}_V^2}{\kappa_V} + \frac{1}{2} + \varepsilon_{1M}^2 + \frac{\varphi_V^2}{\kappa_V} \quad (67)$$

Define the following compact sets

$$\Omega_{z_V} = \left\{ z_V \mid |z_V| \leq \sqrt{\left( \frac{1}{2} + \varepsilon_{1M}^2 + \frac{\varphi_V^2}{\kappa_V} \right) / \left( \lambda_{V,1} - \frac{1}{4} \right)} \right\}$$

$$\Omega_{\tilde{\varphi}_V} = \left\{ \tilde{\varphi}_V \mid |\tilde{\varphi}_V| \leq \sqrt{\left( \frac{1}{2} + \varepsilon_{1M}^2 + \frac{\varphi_V^2}{\kappa_V} \right) / \left( \frac{1}{\kappa_V} \right)} \right\}$$

Let  $\lambda_{V,1} > 1/4$ , it is clear that  $\dot{L}_V < 0$  will be negative if  $z_V \notin \Omega_{z_V}$  or  $\tilde{\varphi}_V \notin \Omega_{\tilde{\varphi}_V}$ . Therefore, the closed-loop velocity subsystem of FAHV is semiglobally uniformly ultimately bounded. The errors  $z_V$  and  $\tilde{\varphi}_V$  eventually converge into the compact sets  $\Omega_{z_V}$  and  $\Omega_{\tilde{\varphi}_V}$ , respectively, and the semi-global uniformity is finally bounded. If  $\lambda_{V,1}$  is large enough and  $\kappa_V$  is small enough, then  $\Omega_{z_V}$  and  $\Omega_{\tilde{\varphi}_V}$  can be arbitrarily small, then the errors  $z_V$  and  $\tilde{\varphi}_V$  can be arbitrarily small. The proof is completed.

In order to further prove the boundedness of tracking error  $\tilde{V}$ , theorem 4 is given.

**Theorem 4:** When the actuator of velocity subsystem is in amplitude saturation, the state variable  $\vartheta_V$  of the error compensation auxiliary system and  $\tilde{V}$  are bounded.

*Proof:* It can be seen from Theorem 3 that  $z_V$  and  $\tilde{\varphi}_V$  are bounded, and since  $k_V \cdot (2/\pi) \cdot \text{atan}(l_V \vartheta_V) < k_V$  is also bounded, then there must be a constant  $B_\Phi \in R$  such that  $|\Phi - \Phi_c| \leq B_\Phi$ .

Select the Lyapunov function as

$$W_V = \frac{1}{2} \vartheta_V^2 \quad (68)$$

Taking time derivative along (68) and substituting it into Eq. (7)

$$\begin{aligned} \dot{W}_V &= \vartheta_V \dot{\vartheta}_V \\ &= -\frac{2k_V \vartheta_V}{\pi} \text{atan}(l_V \vartheta_V) + \lambda_V \vartheta_V (\Phi - \Phi_c) \\ &\leq -\frac{2k_V |\vartheta_V|}{\pi} \text{atan}(l_V \vartheta_V) + \lambda_V |\vartheta_V| B_\Phi \\ &= -\left( \frac{2k_V}{\pi} \text{atan}(l_V \vartheta_V) - \lambda_V B_\Phi \right) |\vartheta_V| \end{aligned} \quad (69)$$

According to  $-\frac{\pi}{2} < \text{atan}(l_V \vartheta_V) < \frac{\pi}{2}$ ,  $\frac{2}{\pi} \text{atan}(l_V \vartheta_V) < 1$  can be obtained. Because  $k_V > 0$ , then  $k_V > \frac{2k_V}{\pi} \text{atan}(l_V \vartheta_V)$ . As long as appropriate  $k_V$ ,  $\lambda_V$  and  $B_\Phi$  are selected, it can be guaranteed that  $k_V > \frac{2k_V}{\pi} \text{atan}(l_V \vartheta_V) > \lambda_V B_\Phi$ ,  $\dot{W}_V < 0$  holds. so the closed-loop system is globally uniformly asymptotically stable, and  $\vartheta_V$  is globally uniformly eventually bounded. At the same time, because  $\tilde{V} = z_V + \vartheta_V$ , then  $\tilde{V}$  is also bounded, and the proof is completed.

## B. STABILITY ANALYSIS OF ALTITUDE SUBSYSTEM

**Theorem 5:** Consider the closed-loop altitude subsystem of FAHV (40), consisting of control law (59), adaptive law (62), STD (2) and the amplitude and rate saturation error compensation auxiliary system (7) under the premise of Theorem 2, then the closed-loop control system is semiglobally uniformly ultimately bounded.

*Proof:* Define estimation error

$$\tilde{\varphi}_h = \hat{\varphi}_h - \varphi_h \quad (70)$$

The estimation errors of STD for  $\chi_2$ ,  $\chi_3$ ,  $\dot{\gamma}_d$ ,  $\ddot{\gamma}_d$  and  $\gamma_d$  are defined as

$$\begin{cases} \tilde{\chi}_2 = \hat{\chi}_2 - \chi_2 \\ \tilde{\chi}_3 = \hat{\chi}_3 - \chi_3 \\ \tilde{\dot{\gamma}}_d = \dot{\hat{\gamma}}_d - \dot{\gamma}_d \\ \tilde{\ddot{\gamma}}_d = \ddot{\hat{\gamma}}_d - \ddot{\gamma}_d \\ \tilde{\gamma}_d = \hat{\gamma}_d - \gamma_d \end{cases} \quad (71)$$

Substituting Eq. (51), Eqs. (59)~(62) into Eq. (58)

$$\begin{aligned} \dot{\hat{z}}_E &= \delta_{e0} - \delta_{e1} + \theta_2^{*T} \xi_2(X_2) + \varepsilon_2 - \hat{\gamma}_d + \frac{2k_1}{\pi} \text{atan}(l_1 \vartheta_1) \\ &\quad + \frac{2k_2}{\pi} \text{atan}(l_2 \vartheta_2) + \frac{2k_3}{\pi} \text{atan}(l_3 \vartheta_3) + 3\tilde{h}\ddot{z}_\gamma + 3\tilde{h}^2\dot{z}_\gamma + \tilde{h}^3 z_\gamma \\ &= -\tau_h \hat{z}_E - \frac{1}{2} \hat{z}_E \hat{\varphi}_h \xi_2^T(X_2) \xi_2(X_2) + \theta_2^{*T} \xi_2(X_2) + \varepsilon_2 \end{aligned} \quad (72)$$

Select the Lyapunov function as

$$L_h = \frac{\hat{z}_E^2}{2} + \frac{\tilde{\varphi}_h^2}{2\kappa_h} \quad (73)$$

Taking time derivative along (73) and substituting (62) and (72) to get

$$\begin{aligned} \dot{L}_h &= \hat{z}_E \dot{\hat{z}}_E + \frac{\tilde{\varphi}_h \dot{\hat{\varphi}}_h}{\kappa_h} = \frac{\tilde{\varphi}_h}{\kappa_h} \left[ \frac{\kappa_h \hat{z}_E^2}{2} \xi_2^T(X_2) \xi_2(X_2) - 2\hat{\varphi}_h \right] \\ &\quad + \hat{z}_E \left[ -\tau_h \hat{z}_E - \frac{1}{2} \hat{z}_E \hat{\varphi}_h \xi_2^T(X_2) \xi_2(X_2) + \theta_2^{*T} \xi_2(X_2) + \varepsilon_2 \right] \\ &= -\tau_h \hat{z}_E^2 - \frac{1}{2} \hat{z}_E^2 \varphi_h \xi_2^T(X_2) \xi_2(X_2) + \hat{z}_E \theta_2^{*T} \xi_2(X_2) \\ &\quad + \varepsilon_2 \hat{z}_E - \frac{2\tilde{\varphi}_h \hat{\varphi}_h}{\kappa_h} \end{aligned} \quad (74)$$

Owing to

$$\begin{aligned} \frac{2\tilde{\varphi}_h \hat{\varphi}_h}{\kappa_h} &\geq \frac{\tilde{\varphi}_h^2}{\kappa_h} - \frac{\varphi_h^2}{\kappa_h}, \hat{z}_E \varepsilon_2 \leq |\hat{z}_E \varepsilon_2| \leq \frac{\hat{z}_E^2}{4} + \varepsilon_{2M}^2 \\ \hat{z}_E \theta_2^{*T} \xi_2(X_2) &\leq \frac{\hat{z}_E^2}{2} \left\| \theta_2^{*T} \xi_2(X_2) \right\|^2 + \frac{1}{2} \\ &= \frac{\hat{z}_E^2}{2} \left\| \theta_2^* \right\|^2 \left\| \xi_2(X_2) \right\|^2 + \frac{1}{2} \\ &= \frac{\hat{z}_E^2}{2} \varphi_h \xi_2^T(X_2) \xi_2(X_2) + \frac{1}{2} \end{aligned}$$

Eq. (74) can be transformed into

$$\dot{L}_h \leq - \left( \tau_h - \frac{1}{4} \right) \hat{z}_E^2 - \frac{\tilde{\varphi}_h^2}{\kappa_h} + \frac{1}{2} + \varepsilon_{2M}^2 + \frac{\varphi_h^2}{\kappa_h} \quad (75)$$

Define the following compact sets

$$\Omega_{\hat{z}_E} = \left\{ \hat{z}_E \mid |\hat{z}_E| \leq \sqrt{\left(\frac{1}{2} + \varepsilon_{2M}^2 + \frac{\varphi_h^2}{\kappa_h}\right) / \left(\tau_h - \frac{1}{4}\right)} \right\}$$

$$\Omega_{\tilde{\varphi}_h} = \left\{ \tilde{\varphi}_h \mid |\tilde{\varphi}_h| \leq \sqrt{\left(\frac{1}{2} + \varepsilon_{2M}^2 + \frac{\varphi_h^2}{\kappa_h}\right) / \left(\frac{1}{\kappa_h}\right)} \right\}$$

Let  $\tau_h > 1/4$ , if  $\hat{z}_E \notin \Omega_{\hat{z}_E}$  or  $\tilde{\varphi}_h \notin \Omega_{\tilde{\varphi}_h}$ , then  $\dot{L}_h < 0$ . Therefore, the closed-loop control system is semiglobally uniformly ultimately bounded. Further, these error signals  $\hat{z}_E$  and  $\tilde{\varphi}_h$  are semiglobally uniformly ultimately bounded and can be invariant to the following sets  $\Omega_{\hat{z}_E}$  and  $\Omega_{\tilde{\varphi}_h}$ . The radiuses of  $\Omega_{\hat{z}_E}$  and  $\Omega_{\tilde{\varphi}_h}$  can be made arbitrarily small by choosing  $\tau_h$  that is large enough and  $\kappa_h$  that is small enough, and the tracking errors  $\hat{z}_E$  and  $\tilde{\varphi}_h$  can also be arbitrarily small. Theorem 5 can be proved.

From Eqs. (54)~(58), we can get

$$\begin{aligned} \dot{\hat{z}}_E &= \ddot{z}_\gamma + 3\dot{h}\dot{z}_\gamma + 3h^2z_\gamma + \dot{h}^3 \int_0^t z_\gamma d\tau \\ &= z_E + (\tilde{\chi}_3 - \tilde{\gamma}_d) + 3\dot{h}(\tilde{\chi}_2 - \tilde{\gamma}_d) - \int_0^t (\tilde{\gamma}_d) d\tau \\ &= z_E + \tilde{\chi}_3 - 2(\tilde{\gamma}_d) + 3\dot{h}(\tilde{\chi}_2 - \tilde{\gamma}_d) \end{aligned} \quad (76)$$

Considering the properties of STD proposed above, there are bounded constants  $\tilde{\chi}_{2M}, \tilde{\chi}_{3M}, \tilde{\gamma}_{dM}, \dot{\tilde{\gamma}}_{dM}$  and  $\tilde{\gamma}_{dM}$  such that  $|\tilde{\chi}_2| \leq \tilde{\chi}_{2M}, |\tilde{\chi}_3| \leq \tilde{\chi}_{3M}, |\tilde{\gamma}_d| \leq \tilde{\gamma}_{dM}, |\dot{\tilde{\gamma}}_d| \leq \dot{\tilde{\gamma}}_{dM}, |\tilde{\gamma}_d| \leq \tilde{\gamma}_{dM}$ , then

$$\begin{aligned} |z_E| &= \left| \hat{z}_E - \left[ \tilde{\chi}_3 - 2(\tilde{\gamma}_d) + 3\dot{h}(\tilde{\chi}_2 - \tilde{\gamma}_d) \right] \right| \\ &\leq |\hat{z}_E| + \tilde{\chi}_{3M} + 2(\tilde{\gamma}_{dM}) + 3\dot{h}(\tilde{\chi}_{2M} - \tilde{\gamma}_{dM}) \end{aligned} \quad (77)$$

Therefore,  $z_E$  and  $z_\gamma$  are also bounded.

**Theorem 6:** When the actuator of altitude subsystem is in amplitude and rate saturation, the state variables  $\vartheta_1, \vartheta_2, \vartheta_3$  of the error compensation auxiliary system and  $e$  are bounded.

**Proof:** Since  $\hat{z}_E, z_E, z_\gamma$  and  $\tilde{\varphi}_h$  are both bounded, the boundedness of the polynomial  $-3\dot{h}\ddot{z}_\gamma - 3h^2\dot{z}_\gamma - \dot{h}^3z_\gamma$  is proved below. According to Eqs. (54)~(58), we can get

$$\begin{aligned} &-3\dot{h}\ddot{z}_\gamma - 3h^2\dot{z}_\gamma - \dot{h}^3z_\gamma \\ &= -3\dot{h}(\ddot{z}_\gamma + \tilde{\chi}_3 - \tilde{\gamma}_d) - 3h^2(\dot{z}_\gamma + \tilde{\chi}_2 - \tilde{\gamma}_d) - \dot{h}^3z_\gamma \\ &\leq -3\dot{h}\ddot{z}_\gamma - 3h^2\dot{z}_\gamma - \dot{h}^3z_\gamma + 3\dot{h}(\tilde{\chi}_{3M} + \tilde{\gamma}_{dM}) \\ &\quad + 3h^2(\tilde{\chi}_{2M} + \tilde{\gamma}_{dM}) \end{aligned} \quad (78)$$

Since the characteristic roots  $-\dot{h}/2 \pm (\sqrt{3}\dot{h}/6)j$  of the polynomial  $-3\dot{h}\ddot{z}_\gamma - 3h^2\dot{z}_\gamma - \dot{h}^3z_\gamma$  have negative real part, the polynomial is Hurwitz and must be bounded.

Owing to

$$\left| -\frac{2k_1}{\pi} \text{atan}(l_1 \vartheta_1) - \frac{2k_2}{\pi} \text{atan}(l_2 \vartheta_2) - \frac{2k_3}{\pi} \text{atan}(l_3 \vartheta_3) \right| < k_1 + k_2 + k_3 \quad (79)$$

Then there must be a constant  $B_{\delta_e} \in R$  such that  $|\delta_e - \delta_{ec}| \leq B_{\delta_e}$ .

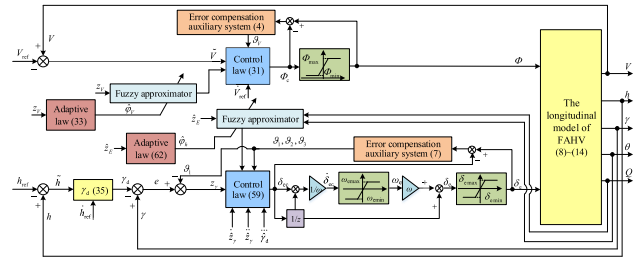


FIGURE 4. Structure of the control system.

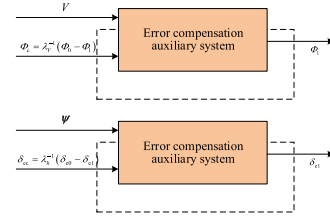


FIGURE 5. Schematic diagram of "algebraic loops".

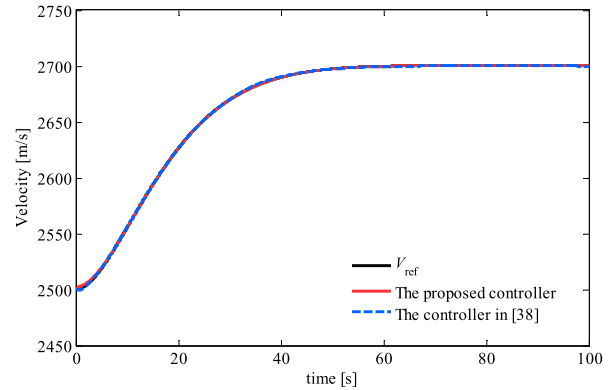


FIGURE 6. Velocity tracking performance.

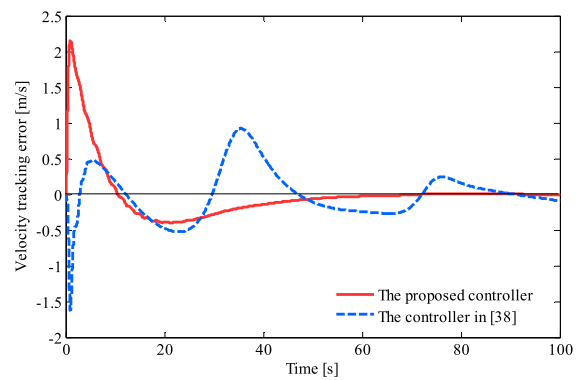


FIGURE 7. Velocity tracking error.

There must be  $\vartheta_i \geq 0 (i = 1, 2, 3)$  in the neighborhood defined near the equilibrium point  $(0, 0, \tan[\lambda_h \pi(\delta_c - \delta_{ec}) / 2k_3] / l_3)$ . Choose the Lyapunov function as

$$W_h = k_2 \int_0^{\vartheta_1} \frac{2}{\pi} \text{atan}(l_1 \tau_1) d\tau_1 + k_2 \int_{\vartheta_1}^{\vartheta_2} \frac{2}{\pi} \text{atan}(l_2 \tau_2) d\tau_2 + \frac{\vartheta_3^2}{2} \quad (80)$$

TABLE 1. Initial trim conditions.

Items	Values	Units
$V$	2500	m/s
$h$	27000	m
$\gamma$	0	deg
$\theta$	1.5295	deg
$Q$	0	Deg/s
$\eta_1$	0.2857	—
$\eta_2$	0.2857	—

TABLE 2. Membership functions of variables.

Items	Membership functions
$V$	$\exp\left\{-\left(\frac{V-i_V}{200}\right)^2\right\}$
$\gamma$	$\exp\left\{-\left(\frac{\gamma-i_\gamma}{0.05}\right)^2\right\}$
$\theta$	$\exp\left\{-\left(\frac{\theta-i_\theta}{0.09}\right)^2\right\}$
$Q$	$\exp\left\{-\left(\frac{Q-i_Q}{0.05}\right)^2\right\}$
$\phi$	$\exp\left\{-\left(\frac{\Phi-i_\Phi}{10}\right)^2\right\}$
$\delta_e$	$\exp\left\{-\left(\frac{\delta_e-i_{\delta_e}}{0.05}\right)^2\right\}$

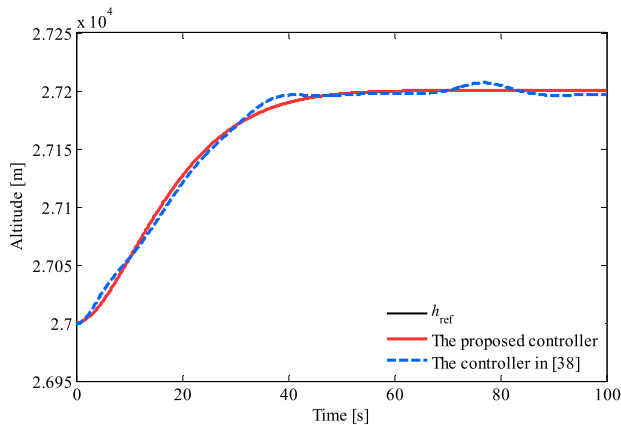


FIGURE 8. Altitude tracking performance.

Taking time derivative along (80)

$$\begin{aligned} \dot{W}_h &= \frac{2k_2}{\pi} \operatorname{atan}(l_1 \vartheta_1) \dot{\vartheta}_1 \\ &+ \left( \frac{2k_2}{\pi} \operatorname{atan}(l_2 \vartheta_2) \dot{\vartheta}_2 - \frac{2k_2}{\pi} \operatorname{atan}(l_1 \vartheta_1) \dot{\vartheta}_1 \right) \\ &+ \vartheta_3 \dot{\vartheta}_3 \end{aligned}$$

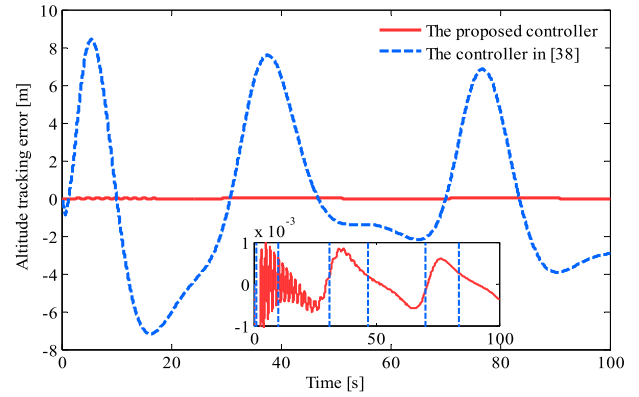


FIGURE 9. Altitude tracking error.

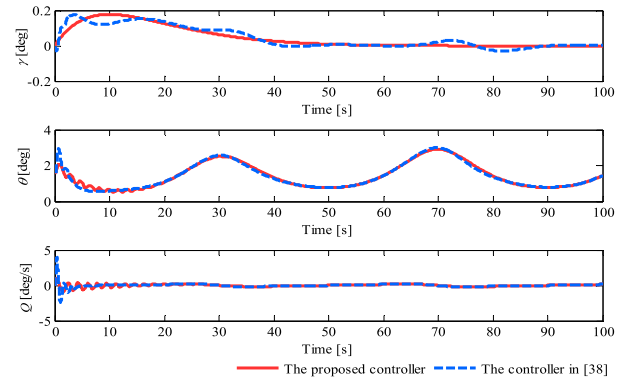


FIGURE 10. The responses of flight-path angle, pitch angle and pitch rate.

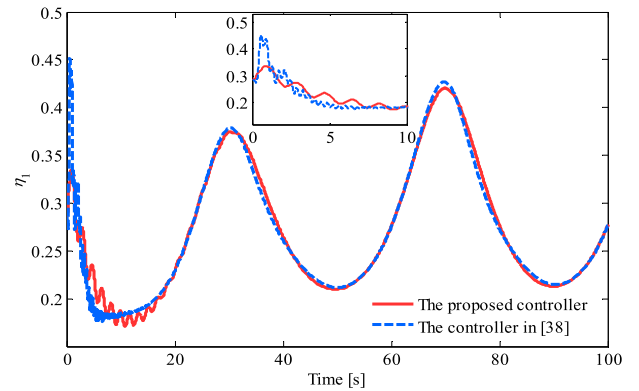


FIGURE 11. The flexible state of  $\eta_1$ .

$$\begin{aligned} &= \frac{2k_2}{\pi} \operatorname{atan}(l_2 \vartheta_2) \vartheta_3 + \vartheta_3 \left[ -\frac{2k_1}{\pi} \operatorname{atan}(l_1 \vartheta_1) - \frac{2k_2}{\pi} \right. \\ &\quad \left. \times \operatorname{atan}(l_2 \vartheta_2) - \frac{2k_3}{\pi} \operatorname{atan}(l_3 \vartheta_3) + \lambda_h (\delta_e - \delta_{ec}) \right] \\ &\leq -\frac{2k_1}{\pi} \operatorname{atan}(l_1 \vartheta_1) \vartheta_3 - \frac{2k_3}{\pi} \operatorname{atan}(l_3 \vartheta_3) \vartheta_3 + \lambda_h B_{\delta_e} |\vartheta_3| \\ &\leq -\frac{2k_3}{\pi} \operatorname{atan}(l_3 \vartheta_3) \vartheta_3 + \lambda_h B_{\delta_e} |\vartheta_3| \\ &\leq -\left( \frac{2k_3}{\pi} \operatorname{atan}(l_3 \vartheta_3) - \lambda_h B_{\delta_e} \right) |\vartheta_3| \end{aligned} \quad (81)$$

If the auxiliary system parameter  $k_3$  satisfies  $k_3 \geq k_3 |2/\pi \cdot \operatorname{atan}(l_3 \vartheta_3)| \geq B_{\delta_e}$ , then  $\dot{W}_h \leq 0$ . At this point,

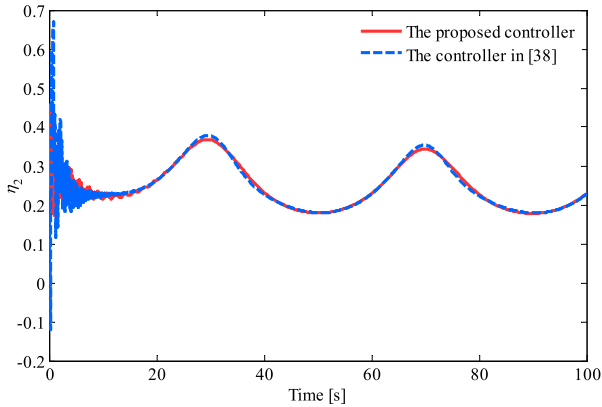


FIGURE 12. The flexible state of  $\eta_2$ .

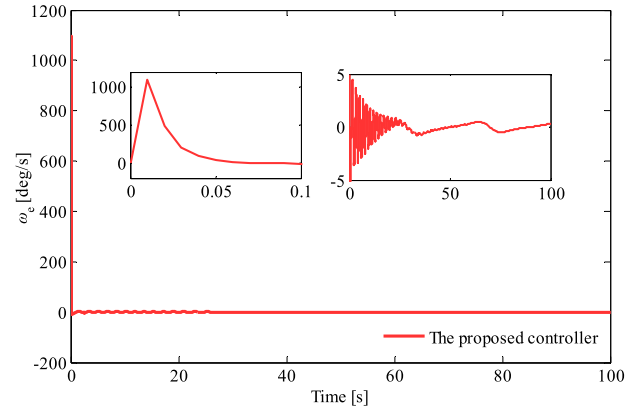


FIGURE 15. The control input  $\omega_e$  of the proposed controller.

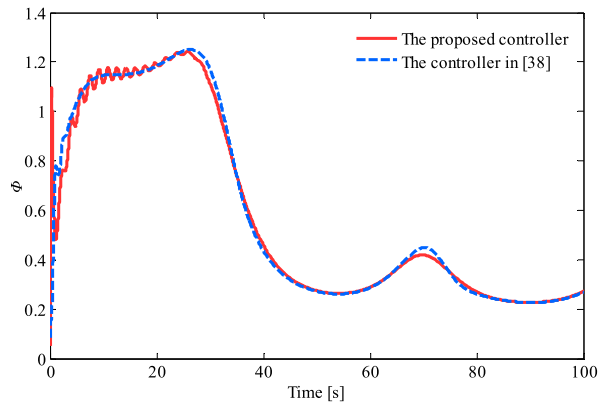


FIGURE 13. The control input  $\phi$ .

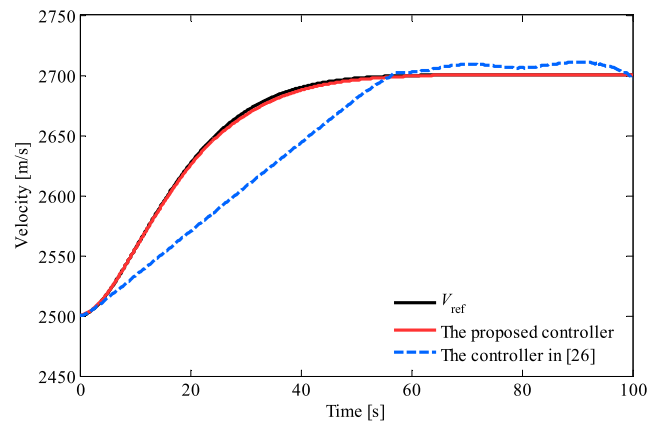


FIGURE 16. Velocity tracking performance.

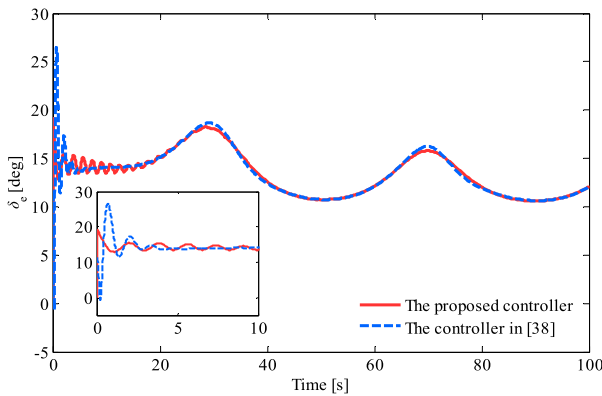


FIGURE 14. The control input  $\delta_e$ .

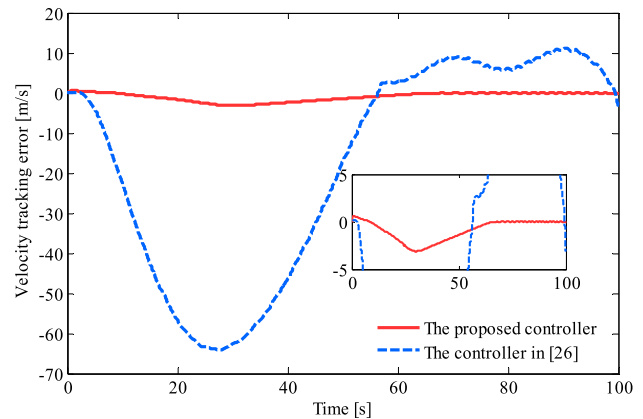


FIGURE 17. Velocity tracking error.

the state variables  $\vartheta_1$ ,  $\vartheta_2$ , and  $\vartheta_3$  are bounded, and the closed-loop system is globally asymptotically stable. And because  $e = z_\gamma + \vartheta_1$ ,  $e$  is also bounded.

The design procedure of velocity and altitude controllers is completed. The structure of the control system is presented in Figure 4.

*Remark 10:* Unlike previous control method, the controller proposed in this paper is designed based on the non-affine models of FAHV, so it has better reliability and practicability.

*Remark 11:* If the input vectors of fuzzy approximators are  $X_1 = [V, \Phi]^T$  and  $X_2 = [\psi^T, \delta_e]^T$ , then  $\Phi_1$  and  $\delta_{e1}$  are both inputs and outputs of fuzzy approximators,

which will produce “algebraic loops” and seriously affect the calculation speed of system. Therefore, in order to avoid algebraic loops, the input vectors in this paper are  $X_1 = [V, \Phi_0]^T$  and  $X_2 = [\psi^T, \delta_{e0}]^T$ , respectively. As shown in Figure 5.

## VI. SIMULATION VERIFICATION

In order to verify the effectiveness of the proposed new control scheme and error compensation auxiliary systems, taking FAHV longitudinal model as the control object to track the reference velocity and reference altitude. The initial

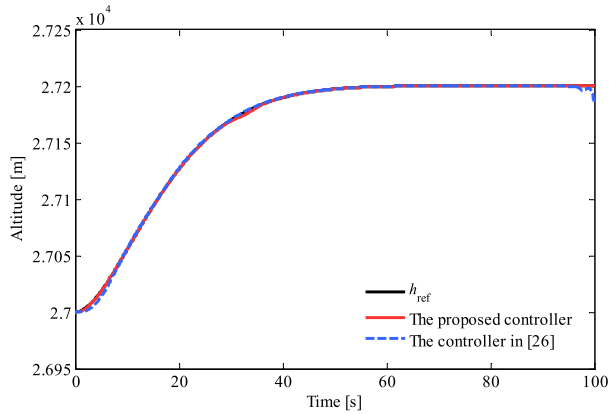


FIGURE 18. Altitude tracking performance.

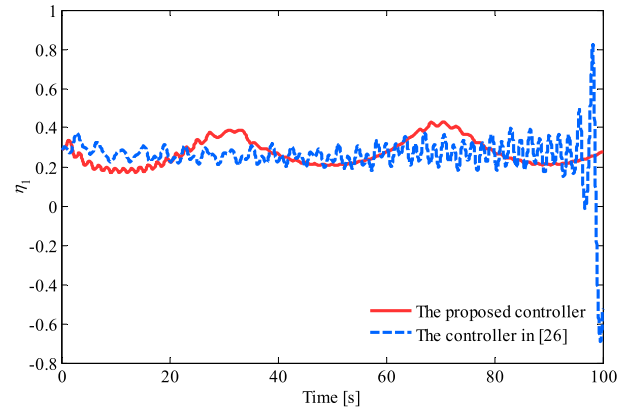


FIGURE 21. The flexible state of  $\eta_1$ .

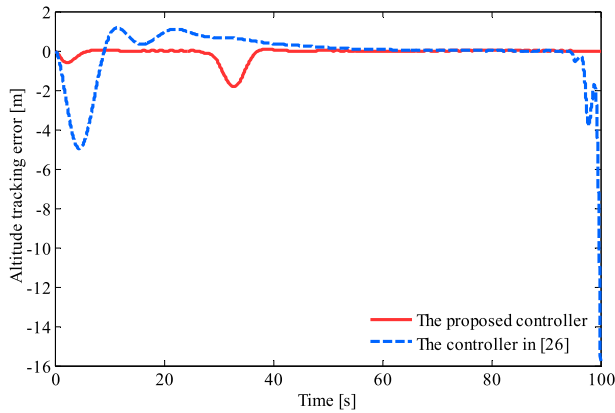


FIGURE 19. Altitude tracking error.

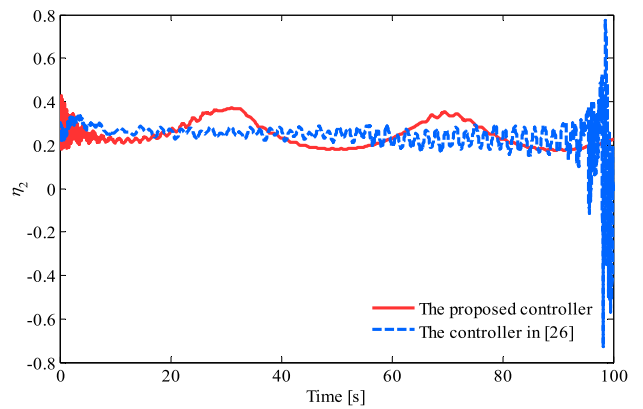


FIGURE 22. The flexible state of  $\eta_2$ .

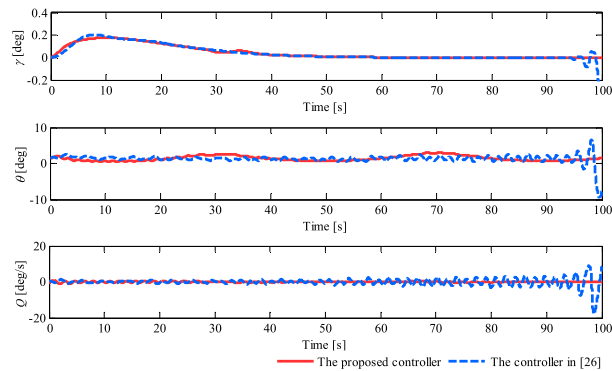


FIGURE 20. The responses of flight-path angle, pitch angle and pitch rate.

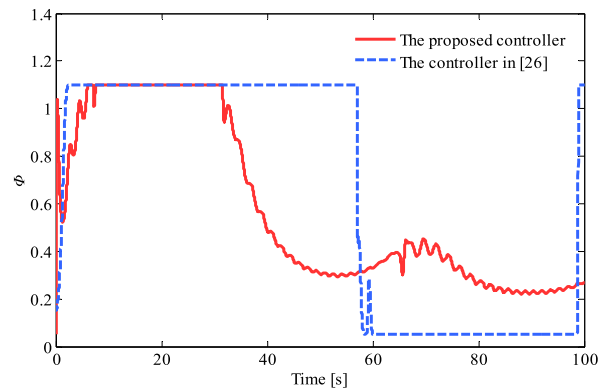


FIGURE 23. The control input  $\phi$ .

trim conditions of FAHV, calculated by employing the Trim Function of MATLAB, are listed in Table 1. The reference velocity input and reference altitude input are given by the second-order reference model, in which the damping ratio is 0.9 and the natural frequency is 0.1 rad/s, the simulation step  $\omega$  is 0.01s.

The design parameters of the controller are  $\lambda_V = 0.9$ ,  $\lambda_{V,1} = 0.3$ ,  $\lambda_{V,2} = 0.8$ ,  $k_h = 2$ ,  $\lambda_h = 0.9$ ,  $\tau_h = 50$ ,  $\bar{h} = 7$ , respectively. The design parameter of STD is  $R = 0.05$ . The design parameters of the adaptive laws are  $\kappa_V = 0.05$  and  $\kappa_h = 0.05$ . The fuzzy approximator choose the Gauss basis function as the membership function, and the fuzzy sets of

each variable to 100. In the velocity subsystem, the input of fuzzy approximator is  $X_1 = [V, \Phi_0]^T$ , The fuzzy centers  $i_V$  and  $i_{\Phi_0}$  of each fuzzy set of  $V$  and  $\Phi_0$  are uniformly distributed in  $[2500m, 2800m]$  and  $[0,2]$ , respectively. In the altitude subsystem, the input vector is  $X_2 = [\gamma, \theta, Q, \delta_{e0}]^T$ , The fuzzy centers  $i_\gamma$ ,  $i_\theta$ ,  $i_Q$  and  $i_{\delta_{e0}}$  of each fuzzy set of  $\gamma$ ,  $\theta$ ,  $Q$  and  $\delta_{e0}$  are uniformly distributed in  $[-1.1^\circ, +1.1^\circ]$ ,  $[0^\circ, 11.5^\circ]$ ,  $[-5.7^\circ/s, +5.7^\circ/s]$  and  $[-23^\circ, +23^\circ]$ , respectively. The membership functions of each variable are given in Table 2. The design parameters of the auxiliary system are  $k_V = 1$ ,  $k_1 = 1$ ,  $k_2 = 1$ ,  $k_3 = 1$ ,  $l_V = 7$ ,  $l_1 = 7$ ,  $l_2 = 7$ ,

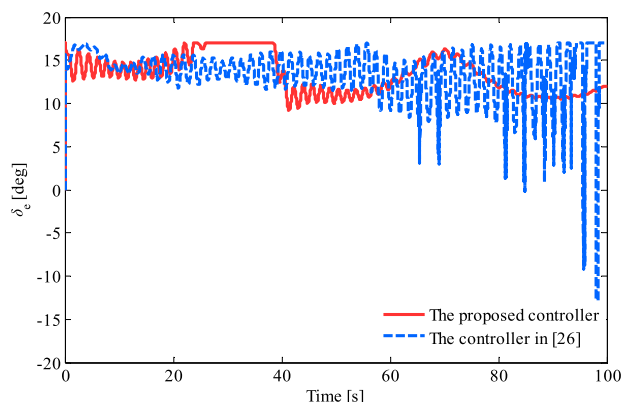


FIGURE 24. The control input  $\delta_e$ .

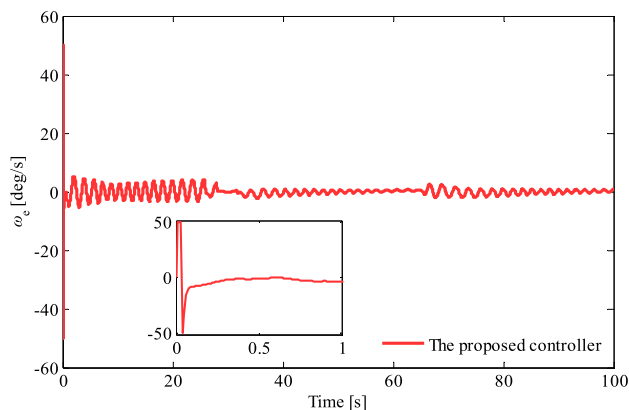


FIGURE 25. The control input  $\omega_e$  of the proposed controller with auxiliary system.

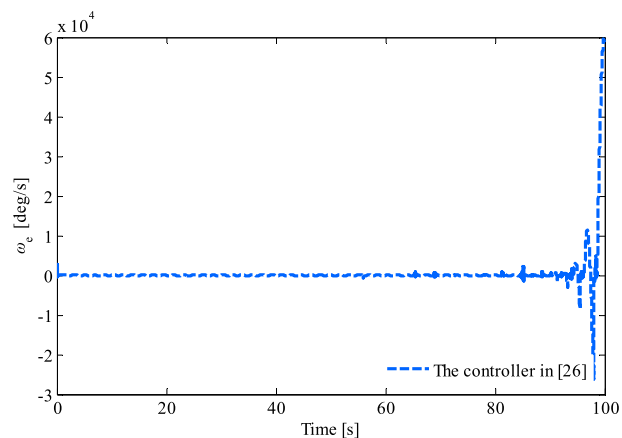


FIGURE 26. The control input  $\omega_e$  of the controller in [26].

$l_3 = 7$ . The simulation is carried out under the following two scenarios.

*Scenario 1:* Firstly, do not limit the executable range of control inputs  $\Phi$  and  $\delta_e$ . The method proposed in this paper is compared with the novel back-stepping control method in [38]. It is assumed that the aerodynamic coefficient of the FAHV model has a perturbation of  $\pm 40\%$ , and the perturbation is  $C = C_0[1 + 0.4 \sin(0.1\pi t)]$ , where  $C_0$  represents the nominal value and  $C$  stands for the simulation value. After the running time exceeds 50 s, the perturbation  $C$  is added.

As can be seen from Figures 6-9, velocity and altitude tracking error converge to zero faster when using the proposed controller than by employing the strategy of [38], and the tracking error of the proposed scheme is significantly smaller than [38], especially the altitude tracking error. It can be seen from Figures 10-12 that the control performance of attitude angles and flexible states of the proposed method is better than the method adopted in [38]. It can be seen from Figure 13-14 that the amplitude of control input of the method proposed in this paper is smaller than the method proposed in [38]. Figure 15 shows that the rate of  $\delta_e$  varies rapidly when the auxiliary system is not adopted. In the next section of the simulation, we consider employing the auxiliary system proposed in this paper to solve the amplitude and rate saturation of the control input.

*Scenario 2:* We assume that actuators are constrained as  $\Phi \in [0.05, 1.1]$ ,  $\delta_e \in [-17^\circ, 17^\circ]$ ,  $\omega_e \in [-50^\circ/s, 50^\circ/s]$ . The method with the auxiliary system proposed in this paper is compared with the method proposed in [26]. After the running time exceeds 50 s, the added perturbation  $C$  is the same as scenario 1.

As can be seen from Figures 16-22, the proposed control scheme can still provide stable tracking of velocity and altitude commands in the presence of control input constraints and parametric uncertainties. And the tracking error is significantly smaller than [26]. The control performance of attitude angle and flexible states is better than [26]. Figures 23-26 shows that the simulation performance of proposed control scheme is better than the controller in [26] under stricter constraints and the proposed method can provide stable tracking with rate saturation of  $\delta_e$ . Since the adopted method in [26] does not take rate saturation into account, it is likely to lead to control failure.

## VII. CONCLUSION

A fuzzy-approximation-based nonlinear tracking control approach is presented for non-affine models of FAHV without many virtual control laws. It avoids the loss of some key dynamics when the models are simplified. Since there is no virtual control law and intermediate variable, the problem of excessive calculation caused by multiple differentiation is avoided. Norm estimation approach is introduced into the fuzzy approximator to improve the efficiency of weight updating. A novel error compensation auxiliary system with multiple constraints is designed to solve the amplitude and rate saturation of the actuator. In the presence of parametric uncertainties, external disturbances and control input constraints, robust tracking of reference trajectories can be achieved by the proposed control strategy with auxiliary systems effectively.

## REFERENCES

- [1] J. J. Bertin and R. M. Cummings, "Fifty years of hypersonics: Where we've been, where we're going," *Prog. Aerosp. Sci.*, vol. 39, nos. 6-7, pp. 511-536, Aug./Oct. 2003.
- [2] X. Bu, "Air-breathing hypersonic vehicles funnel control using neural approximation of non-affine dynamics," *IEEE/ASME Trans. Mechatronics*, vol. 23, no. 5, pp. 2099-2108, Oct. 2018.

- [3] B. Xu and Z. Shi, "An overview on flight dynamics and control approaches for hypersonic vehicles," *Sci. China Inf. Sci.*, vol. 58, no. 7, pp. 1–19, Jul. 2015.
- [4] H. An, F. Baris, J. Liu, C. Wang, and L. Wu, "Adaptive fault-tolerant control of air-breathing hypersonic vehicles robust to input nonlinearities," *Int. J. Control*, vol. 92, no. 5, pp. 1044–1060, 2019.
- [5] G. Chao, H.-N. Wu, B. Luo, and L. Guo, "H-infinity control for air-breathing hypersonic vehicle based on online simultaneous policy update algorithm," *Int. J. Intell. Comput. Cybern.*, vol. 6, no. 2, pp. 126–143, 2013.
- [6] H.-N. Wu, Z.-Y. Liu, and L. Guo, "Robust  $L_\infty$ -gain fuzzy disturbance observer-based control design with adaptive bounding for a hypersonic vehicle," *IEEE Trans. Fuzzy Syst.*, vol. 22, no. 6, pp. 1401–1412, Dec. 2014.
- [7] R. Zhang, C. Sun, J. Zhang, and Y. Zhou, "Second-order terminal sliding mode control for hypersonic vehicle in cruising flight with sliding mode disturbance observer," *J. Control Theory Appl.*, vol. 11, no. 2, pp. 299–305, May 2013.
- [8] H. Gao and Y. Cai, "Sliding mode predictive control for hypersonic vehicle," *J. Xian Jiaotong Univ.*, vol. 48, no. 1, pp. 67–72, Jan. 2014.
- [9] C. Chen, G. Ma, Y. Sun, and C. Li, "Recursive sliding mode control for hypersonic vehicle based on nonlinear disturbance observer," *Acta Armamentarii*, vol. 37, no. 5, pp. 840–850, 2016.
- [10] H. An, J. Liu, C. Wang, and L. Wu, "Approximate back-stepping fault-tolerant control of the flexible air-breathing hypersonic vehicle," *IEEE/ASME Trans. Mechatronics*, vol. 21, no. 3, pp. 1680–1691, Jun. 2016.
- [11] X. Bu, G. He, and D. Wei, "A new prescribed performance control approach for uncertain nonlinear dynamic systems via back-stepping," *J. Franklin Inst.*, vol. 355, no. 17, pp. 8510–8536, Nov. 2018.
- [12] B. Xu and Y. Zhang, "Neural discrete back-stepping control of hypersonic flight vehicle with equivalent prediction model," *Neurocomputing*, vol. 154, pp. 337–346, Apr. 2015.
- [13] P. Wang, W. Jie, X. Bu, L. Chang, and S. Tan, "Adaptive fuzzy back-stepping control of a flexible air-breathing hypersonic vehicle subject to input constraints," *J. Intell. Robot. Syst.*, vol. 87, nos. 3–4, pp. 565–582, Sep. 2017.
- [14] Y. Liu, Z. Pu, and J. Yi, "Observer-based robust adaptive T2 fuzzy tracking control for flexible air-breathing hypersonic vehicles," *IET Control Theory Appl.*, vol. 12, no. 8, pp. 1036–1045, May 2018.
- [15] D. X. Gao, Z. Q. Sun, X. Luo, and T. R. Du, "Fuzzy adaptive control for hypersonic vehicle via backstepping method," *Control Theory Appl.*, vol. 25, no. 5, pp. 805–810, 2008.
- [16] X. Bu, X. Wu, J. Huang, Z. Ma, and R. Zhang, "Minimal-learning-parameter based simplified adaptive neural back-stepping control of flexible air-breathing hypersonic vehicles without virtual controllers," *Neurocomputing*, vol. 175, pp. 816–825, Jan. 2016.
- [17] X. Bu, G. He, and K. Wang, "Tracking control of air-breathing hypersonic vehicles with non-affine dynamics via improved neural back-stepping design," *ISA Trans.*, vol. 75, pp. 88–100, Apr. 2018.
- [18] X. Bu, "Guaranteeing prescribed performance for air-breathing hypersonic vehicles via an adaptive non-affine tracking controller," *Acta Astronautica*, vol. 151, pp. 368–379, Oct. 2018.
- [19] L. Fiorentini, A. Serrani, M. A. Bolender, and D. B. Doman, "Nonlinear robust adaptive control of flexible air-breathing hypersonic vehicles," *J. Guid., Control, Dyn.*, vol. 32, no. 2, pp. 402–417, 2009.
- [20] X. Bu, X. Wu, Z. Ma, and R. Zhang, "Nonsingular direct neural control of air-breathing hypersonic vehicle via back-stepping," *Neurocomputing*, vol. 153, pp. 164–173, Apr. 2015.
- [21] Y. Wang, C. Jiang, and Q. Wu, "Attitude tracking control for variable structure near space vehicles based on switched nonlinear systems," *Chin. J. Aeronaut.*, vol. 26, no. 1, pp. 186–193, Feb. 2013.
- [22] Y. Hou, C. Dong, and Q. Wang, "Stability analysis of switched linear systems with locally overlapped switching law," *J. Guid., Control, Dyn.*, vol. 33, no. 2, pp. 396–403, Mar. 2010.
- [23] C. Dong, Y. Hou, and Q. Wang, "Model reference adaptive switching control of a linearized hypersonic flight vehicle model with actuator saturation," *Proc. Inst. Mech. Eng., I, J. Syst. Control Eng.*, vol. 224, no. 3, pp. 289–303, May 2010.
- [24] X. Bu, X. Wu, Z. Ma, R. Zhang, and J. Huang, "Novel auxiliary error compensation design for the adaptive neural control of a constrained flexible air-breathing hypersonic vehicle," *Neurocomputing*, vol. 171, pp. 313–324, Jan. 2016.
- [25] H. An, J. Liu, C. Wang, and L. Wu, "Disturbance observer-based anti-windup control for air-breathing hypersonic vehicles," *IEEE Trans. Ind. Electron.*, vol. 63, no. 5, pp. 3038–3049, May 2016.
- [26] C. Luo, H. Lei, D. Zhang, and X. Zou, "Adaptive neural control of hypersonic vehicles with actuator constraints," *Int. J. Aerosp. Eng.*, vol. 2018, Jul. 2018, Art. no. 1284753.
- [27] H. An, H. Xia, and C. Wang, "Finite-time output tracking control for air-breathing hypersonic vehicles with actuator constraints," *Proc. Inst. Mech. Eng., G, J. Aerosp. Eng.*, vol. 231, no. 14, pp. 2578–2593, Dec. 2017.
- [28] C. Wang and Y. Lin, "Multivariable adaptive backstepping control: A norm estimation approach," *IEEE Trans. Autom. Control*, vol. 57, no. 4, pp. 989–995, Apr. 2012.
- [29] J.-H. Park, S.-H. Huh, S.-H. Kim, S.-J. Seo, and G.-T. Park, "Direct adaptive controller for nonaffine nonlinear systems using self-structuring neural networks," *IEEE Trans. Neural Netw.*, vol. 16, no. 2, pp. 414–422, Mar. 2005.
- [30] L.-X. Wang and J. M. Mendel, "Fuzzy basis functions, universal approximation, and orthogonal least-squares learning," *IEEE Trans. Neural Netw.*, vol. 3, no. 5, pp. 807–814, Sep. 1992.
- [31] L.-X. Wang, "Stable adaptive fuzzy control of nonlinear systems," *IEEE Trans. Fuzzy Syst.*, vol. 1, no. 2, pp. 146–155, May 2002.
- [32] Z. Yao and H. Cao, "A novel tracking differentiator with good stability and rapidity and its application," *Trans. Beijing Inst. Technol.*, vol. 38, no. 8, pp. 861–867, 2018.
- [33] M. A. Bolender and D. B. Doman, "Nonlinear longitudinal dynamical model of an air-breathing hypersonic vehicle," *J. Spacecraft Rockets*, vol. 44, no. 2, pp. 374–387, Mar. 2007.
- [34] J. T. Parker, A. Serrani, S. Yurkovich, M. A. Bolender, and D. B. Doman, "Control-oriented modeling of an air-breathing hypersonic vehicle," *J. Guid., Control, Dyn.*, vol. 30, no. 3, pp. 856–869, 2007.
- [35] A. J. Calise, N. Hovakimyan, and M. Idan, "Adaptive output feedback control of nonlinear systems using neural networks," *Automatica*, vol. 37, no. 8, pp. 1201–1211, Aug. 2001.
- [36] C. Hu, X. Zhou, B. Sun, W. Liu, and Q. Zong, "Nussbaum-based fuzzy adaptive nonlinear fault-tolerant control for hypersonic vehicles with diverse actuator faults," *Aerosp. Sci. Technol.*, vol. 71, pp. 432–440, Dec. 2017.
- [37] Q. Zong, F. Wang, B. Tian, and R. Su, "Robust adaptive dynamic surface control design for a flexible air-breathing hypersonic vehicle with input constraints and uncertainty," *Nonlinear Dyn.*, vol. 78, no. 1, pp. 289–315, Oct. 2014.
- [38] X. Bu, X. Wu, R. Zhang, Z. Ma, and J. Huang, "Tracking differentiator design for the robust backstepping control of a flexible air-breathing hypersonic vehicle," *J. Franklin Inst.*, vol. 352, no. 4, pp. 1739–1765, Apr. 2015.



**XINGGE LI** received the B.S. degree in vehicle support engineering from the Wuhan University of Technology, in 2013. He is currently pursuing the M.S. degree in control science and engineering with Air Force Engineering University. He was involved in the guidance and the intelligent control of air-breathing hypersonic vehicles.



**GANG LI** received the B.S. degree in high-frequency systems from Air Force Engineering University, in 1984, and the M.S. and Ph.D. degrees in automatic control theory and applications from Xi'an Jiaotong University, in 1992 and 1996, respectively, where he is currently a Professor of control science and engineering. His research interests include the control theory and the applications of aircraft and theory, and the method of intelligent control.

• • •